

# Hypomorphic homozygous mutations in phosphoglucomutase 3 (*PGM3*) impair immunity and increase serum IgE levels

Atfa Sassi, PhD,<sup>a,\*</sup> Sandra Lazaroski, PhD,<sup>b,\*</sup> Gang Wu, MSc,<sup>c,\*</sup> Stuart M. Haslam, PhD,<sup>c</sup> Manfred Fliegauf, PhD,<sup>b</sup> Fethi Mellouli, MD,<sup>d</sup> Turkan Patiroglu, MD,<sup>e,f</sup> Ekrem Unal, MD,<sup>e</sup> Mehmet Akif Ozdemir, MD,<sup>e</sup> Zineb Jouhadi, MD,<sup>g</sup> Khadija Khadir, MD,<sup>g</sup> Leila Ben-Khemis, MSc,<sup>a</sup> Meriem Ben-Ali, PhD,<sup>a</sup> Imen Ben-Mustapha, MD,<sup>a</sup> Lamia Borchan, PhD,<sup>h</sup> Dietmar Pfeifer, PhD,<sup>i</sup> Thilo Jakob, MD,<sup>j</sup> Monia Khemiri, MD,<sup>k</sup> A. Charlotta Asplund, BSc,<sup>l</sup> Manuela O. Gustafsson, MSc,<sup>l</sup> Karin E. Lundin, PhD,<sup>l</sup> Elin Falk-Sörqvist, MSc,<sup>m</sup> Lotte N. Moens, PhD,<sup>m</sup> Hatice Eke Gungor, MD,<sup>f</sup> Karin R. Engelhardt, PhD,<sup>n</sup> Magdalena Dziadzio, MD, PhD,<sup>n</sup> Hans Stauss, MD, PhD,<sup>n</sup> Bernhard Fleckenstein, MD,<sup>o</sup> Rebecca Meier, BSc,<sup>b</sup> Khairunnadiya Prayitno, MSc,<sup>b</sup> Andrea Maul-Pavicic, PhD,<sup>b</sup> Sandra Schaffer,<sup>b</sup> Mirzokhid Rakhmanov, PhD,<sup>b</sup> Philipp Henneke, MD,<sup>b</sup> Helene Kraus, MSc,<sup>b</sup> Hermann Eibel, PhD,<sup>b</sup> Uwe Kölsch, MD,<sup>p</sup> Sellama Nadifi, PhD,<sup>q</sup> Mats Nilsson, PhD,<sup>m</sup> Mohamed Bejaoui, MD,<sup>d</sup> Alejandro A. Schäffer, PhD,<sup>r,\*</sup> C. I. Edvard Smith, MD, PhD,<sup>l,\*</sup> Anne Dell, PhD,<sup>c,\*</sup> Mohamed-Ridha Barbouche, MD, PhD,<sup>a,\*</sup> and Bodo Grimbacher, MD<sup>b,n,\*</sup>

Tunis, Tunisia, Freiburg, Erlangen, and Berlin, Germany, London, United Kingdom, Kayseri,

Turkey, Casablanca, Morocco, Huddinge and Uppsala, Sweden, and Bethesda, Md

**Background:** Recurrent bacterial and fungal infections, eczema, and increased serum IgE levels characterize patients with the hyper-IgE syndrome (HIES). Known genetic causes for HIES are mutations in signal transducer and activator of transcription 3 (*STAT3*) and dedicator of cytokinesis 8 (*DOCK8*), which are involved in signal transduction pathways. However, glycosylation defects have not been described in patients with HIES. One crucial enzyme in the glycosylation pathway is phosphoglucomutase 3 (*PGM3*), which catalyzes a key step in the synthesis of uridine diphosphate N-acetylglucosamine, which is required for the biosynthesis of N-glycans.

**Objective:** We sought to elucidate the genetic cause in patients with HIES who do not carry mutations in *STAT3* or *DOCK8*.

**Methods:** After establishing a linkage interval by means of SNPchip genotyping and homozygosity mapping in 2 families with HIES from Tunisia, mutational analysis was performed with selector-based, high-throughput sequencing. Protein expression was analyzed by means of Western blotting, and glycosylation was profiled by using mass spectrometry.

**Results:** Mutational analysis of candidate genes in an 11.9-Mb linkage region on chromosome 6 shared by 2 multiplex families identified 2 homozygous mutations in *PGM3* that segregated

From <sup>a</sup>the Laboratory of Immunopathology, Vaccinology and Molecular Genetics, Pasteur Institute of Tunis and University Tunis El Manar; <sup>b</sup>the Center for Chronic Immunodeficiency (CCI), <sup>c</sup>the Department of Medicine I, Specialties: Hematology, Oncology, and Stem-Cell Transplantation, and <sup>j</sup>the Allergy Research Group, Department of Dermatology, University Medical Center Freiburg; <sup>d</sup>the Department of Life Sciences, Imperial College London; <sup>d</sup>the Pediatrics Department, Bone Marrow Transplantation Center, Tunis; <sup>e</sup>the Department of Pediatrics, Division of Pediatric Hematology and Oncology, and <sup>f</sup>the Department of Pediatrics, Division of Pediatric Immunology, Faculty of Medicine, Erciyes University, Kayseri; <sup>g</sup>the Department of Pediatric Infectious Diseases, CHU IBN ROCHD, and <sup>h</sup>the Department of Genetics, Hassan II University, Casablanca; <sup>h</sup>the Laboratory of Venoms and Therapeutic Molecules, Institut Pasteur de Tunis; <sup>i</sup>Pediatrics Department A, Children's Hospital of Tunis; <sup>i</sup>the Clinical Research Center, Department of Laboratory Medicine, Karolinska Institutet, Karolinska University Hospital Huddinge; <sup>m</sup>the Department of Immunology, Genetics and Pathology, Uppsala University, Rudbeck Laboratory, Uppsala; <sup>n</sup>the Royal Free Hospital, Institute of Immunity & Transplantation, University College London; <sup>o</sup>the Institute of Virology, Friedrich-Alexander-Universität Erlangen-Nürnberg, Erlangen; <sup>p</sup>the Division of Immunology, Labor Berlin and Institute of Medical Immunology, Charité, Campus Virchow Klinikum, Berlin; and <sup>q</sup>the National Center for Biotechnology Information, National Institutes of Health, Department of Health and Human Services, Bethesda.

\*These authors contributed equally to this work.

Supported by the German Federal Ministry of Education and Research (BMBF 01 EO 0803). The research was supported in part by the Intramural Research Program of the National Library of Medicine—National Institutes of Health. Parts of the study were supported by the Tunisian Ministry for Higher Education and Research, the Swedish Medical Research Council, the Swedish Cancer Society and the Stockholm County Council (research grant ALF), and the European Community's 6th and 7th Framework Programs FP7/2007-2013 under grant agreement

Health-F5-2008-223292 (Euro-Gene-Scan). This work was also supported by the Biotechnology and Biological Sciences Research Council (BBF0083091 and BB/K016164/1 to A.D. and S.M.H.). G.W. is grateful for a Sun Hung Kai Properties-Kwoks' Foundation-Imperial College PhD Scholarship.

Disclosure of potential conflict of interest: S. M. Haslam and A. Dell have received research support from the Biotechnology and Biological Sciences Research Council. L. Ben-Khemis, M. Ben-Ali, I. Ben-Mustapha, M. Khemiri, and M.-R. Barbouche have received research support from the Tunisian Ministry for Higher Education and Research. T. Jakob has consultant arrangements with Allergopharma, Novartis, Jansen Cilag, and Thermo Fisher Scientific; receives research support from Allergopharma, Thermo Fisher Scientific, Birken AG, and Cosmetic Europe; and has received payment for lectures from Stallergenes, ALK-Abelló, Allergies Therapeutics, Novartis, and Thermo Fisher Scientific. A. C. Asplund, M. O. Gustafsson, K. E. Lundin, and C. I. E. Smith have received research support and travel support from the European Union Framework Programme 7. H. Stauss has received research support from Leukemia & Lymphoma Research, has consultant arrangements with Cell Medica, has a patent for Allo-restricted cells, and receives royalties for that patent. B. Fleckenstein has received research support from DFG. B. Grimbacher has received research support from the BMBF, the European Union, and the Helmholtz Society; and has received payment for lectures from CSL, Baxter, and Biotest. The rest of the authors declare that they have no relevant conflicts of interest.

Received for publication July 1, 2013; revised January 31, 2014; accepted for publication February 4, 2014.

Available online April 7, 2014.

Corresponding author: Bodo Grimbacher, MD, Center for Chronic Immunodeficiency (CCI), University Medical Center Freiburg, Engesserstraße 4, 79108 Freiburg, Germany. E-mail: [bodo.grimbacher@uniklinik-freiburg.de](mailto:bodo.grimbacher@uniklinik-freiburg.de). 0091-6749

<http://dx.doi.org/10.1016/j.jaci.2014.02.025>

with disease status and followed recessive inheritance. The mutations predict amino acid changes in PGM3 (p.Glu340del and p.Leu83Ser). A third homozygous mutation (p.Asp502Tyr) and the p.Leu83Ser variant were identified in 2 other affected families, respectively. These hypomorphic mutations have an effect on the biosynthetic reactions involving uridine diphosphate N-acetylglucosamine. Glycomic analysis revealed an aberrant glycosylation pattern in leukocytes demonstrated by a reduced level of tri-antennary and tetra-antennary N-glycans. T-cell proliferation and differentiation were impaired in patients. Most patients had developmental delay, and many had psychomotor retardation.

**Conclusion:** Impairment of *PGM3* function leads to a novel primary (inborn) error of development and immunity because biallelic hypomorphic mutations are associated with impaired glycosylation and a hyper-IgE-like phenotype. (J Allergy Clin Immunol 2014;133:1410-9.)

**Key words:** Hyper-IgE syndrome, glycosylation, *Staphylococcus aureus*, signal transducer and activator of transcription 3, dedicator of cytokinesis 8, phosphoglucomutase 3

Primary immunodeficiencies (PIDs) are rare diseases arising from inborn errors of immunity that often follow Mendelian inheritance.<sup>1</sup> To date, disease-causing mutations in more than 200 genes have been discovered in patients with PIDs (<http://www.iuisonline.org/iuis/index.php/primary-immunodeficiency-expert-committee.html>). These can affect the expression, function, or both of proteins involved in various innate and adaptive

#### Abbreviations used

AD:	Autosomal dominant
AR:	Autosomal recessive
CDG:	Congenital disorder of glycosylation
DOCK8:	Dedicator of cytokinesis 8
FACS:	Fluorescence-activated cell sorting
FITC:	Fluorescein isothiocyanate
FLAER:	Fluorescently labeled aerolysin binding tightly and specifically to mammalian GPI anchors
GIP:	Glycosyl-phosphatidylinositol
GlcNAc-1-P:	N-acetyl-D-glucosamine-1-phosphate
GlcNAc-6-P:	N-acetyl-D-glucosamine-6-phosphate
HIES:	Hyper-IgE syndrome
Km:	Michaelis-Menten constant
LOD:	Logarithm of odds
PGM3:	Phosphoglucomutase 3
PID:	Primary immunodeficiency
PMA:	Phorbol 12-myristate 13-acetate
STAT3:	Signal transducer and activator of transcription 3
UDP-GlcNAc:	Uridine diphosphate N-acetylglucosamine

immunologic processes.<sup>2,3</sup> In patients with one of these PIDs, termed hyper-IgE syndrome (HIES), monogenic defects have been detected in signal transducer and activator of transcription 3 (*STAT3*), dedicator of cytokinesis 8 (*DOCK8*), and tyrosine kinase 2 (*TYK2*),<sup>4-8</sup> which encode proteins with pivotal roles in signal transduction pathways in immune cells.

Congenital disorders of glycosylation (CDGs) have been described to lead to PIDs because accurate glycosylation of

**TABLE I.** Clinical findings in patients with HIES with homozygous *PGM3* mutations

	Patient								
	A.V.12	A.V.13	A.V.14	A.V.18	B.V.6	B.V.7	C.IV.7	D.IV.2	D.IV.5
Origin	Tunisia	Tunisia	Tunisia	Tunisia	Tunisia	Tunisia	Turkey	Morocco	Morocco
Sex	M	F	F	M	M	M	M	M	M
Age of onset	4 mo	7 mo	2 mo	1 mo	3 mo	4 mo	6.5 y	3 mo	3 mo
Age at last evaluation/death	7 y	Deceased: 14 mo	Deceased: 13 mo	6 y, 2 mo	34 y	32 y	11.5 y	21 y	11 y
<i>PGM3</i> mutation	p.E340del	p.E340del	p.E340del	p.E340del	p.L83S	p.L83S	p.D502Y	p.L83S	p.L83S
Symptoms typical for HIES									
Recurrent RTI	Yes	Yes	Yes	Yes	Yes	Yes	Yes	Yes	Yes
Pneumonias	3	3	3	2	>3	>3	3	>3	3
Lung abnormalities (bronchiectasis)	Yes	No	No	No	Yes	Yes	Yes	Yes	Yes
Eczema	Moderate	Severe	Severe	Severe	Severe	Severe	No	Severe	No
Abscesses	Yes	Yes	Yes	Yes	Yes	Yes	No	Yes (cold)	No
Candidiasis	Oral	Oral	Oral	Ear	Fingernails	Oral	No	No	No
Viral infections	No	RSV	RSV	No	No	No	Severe VZV	Yes	No
<i>Staphylococcus aureus</i> infections	Yes	Yes	Yes	Yes	Yes	Yes	Yes	Yes	No
Characteristic facies	No	No	No	No	Yes	Yes	No	Yes	Yes
Hyperextensibility	No	No	No	Yes	Yes	Yes	No	No	No
Serum IgE (IU/mL)	18,730	7,174	3,029	16,534	99,600	141,300	9,320	>17,000	>18,500
Eosinophilia	Yes	Yes	Yes	Yes	Yes	Yes	Yes	Yes	Yes
HIES score	50	45	48	47	56	53	27	55	43
Symptoms found in both patients with HIES and patients with CDG									
Failure to thrive	Yes	Yes	Yes	Yes	Yes	Yes	No	Yes	No
Scoliosis	Yes	No	No	No	No	No	No	No	No
Symptoms typical for CDG									
Developmental delay	Yes	NA	NA	Yes	Mild	Mild	Yes	Mild	No
Psychomotor retardation	Yes	NA	NA	Yes	No	No	No	Yes	No
Hypotonia	Severe	NA	NA	Severe	No	No	No	Yes	No

F, Female; M, male; NA, not applicable; RTI, respiratory tract infection.

**TABLE II.** Laboratory findings in patients with HIES with homozygous *PGM3* mutations

	Patients		
	A.V.12	A.V.13	A.V.14
Age at measurement	7 y	11 mo	11 mo
Cell counts/ $\mu$ L			
WBC	6,300 (4,400-9,500)	11,600 (6,400-13,000)	4,606 ↓ (6,400-13,000)
ANC	1,510 ↓ (1,700-7,000)	6,100 (2,000-8,000)	950 ↓ (2,000-8,000)
ALC	3,530 (1,900-3,700)	4,100 (3,400-9,000)	1,940 ↓ (3,400-9,000)
AEC	760 ↑ (100-600)	1,540 ↑ (50-600)	700 ↑ (50-600)
PLT ( $\times$ 1,000)	ND (130-400)	230 (130-400)	150 (130-400)
Lymphocyte subsets (%)			
CD3	69.5 (60-76)	26 ↓ (49-76)	74 (49-76)
CD4	13.5 ↓ (31-47)	8 ↓ (31-56)	18.5 ↓ (31-56)
CD8	56.5 ↑ (18-35)	34 ↑ (12-24)	53 ↑ (12-24)
CD4/CD8	0.24 (1.34-1.72)	0.24 (2.33-2.58)	0.35 (2.33-2.58)
CD19	9 ↓ (13-27)	18.5 (14-37)	8.5 ↓ (14-37)
NK (CD3 <sup>-</sup> CD16 <sup>+</sup> CD56 <sup>+</sup> )	25 ↑ (4-17)	52.5 ↑ (3-15)	18.5 ↑ (3-15)
Lymphocyte subsets (counts/ $\mu$ L)			
CD3	2,450 (2,120-2,680)	1,066 ↓ (2,000-3,120)	1,435 ↓ (2,000-3,120)
CD4	476 ↓ (1,100-1,700)	328 ↓ (1,270-2,300)	360 ↓ (1,270-2,300)
CD8	1,994 ↑ (635-1,235)	1,394 ↑ (492-984)	1,030 ↑ (492-984)
CD19	318 ↓ (460-950)	760 (574-1,520)	165 ↓ (574-1,520)
NK (CD3 <sup>-</sup> CD16 <sup>+</sup> CD56 <sup>+</sup> )	880 ↑ (141-600)	2,150 ↑ (123-615)	360 (123-615)
Serum immunoglobulins			
IgM (g/L)	1.74 (0.75-1.97)	2.25 ↑ (0.4-1.9)	3.93 ↑ (0.4-1.9)
IgG (g/L)	5.80 (5-17)	19.03 ↑ (5-11)	16.38 ↑ (5-11)
IgA (g/L)	1.41 (0.85-2.2)	2.31 ↑ (0.55-1.2)	1.25 ↑ (0.55-1.2)
IgE (IU/mL)	18,730 ↑ (0-200)	7,174 ↑ (0-200)	3,029 ↑ (0-200)
NBT	Normal	Normal	Normal

Arrows indicate values greater than (↑) or less than (↓) the reference ranges. Normal ranges are from the 10th to 90th percentiles.<sup>21</sup>

AEC, Absolute erythrocyte counts; ALC, absolute lymphocyte count; ANC, absolute neutrophil count; NBT, Nitro Blue Tetrazolium test; ND, not done; NK, natural killer; PLT, platelets; WBC, white blood count.

most immune receptors, immunoglobulins, proteins of the complement, and cytokines is essential for the integrity of immune function.<sup>9,10</sup> Profound hypoglycosylation of *N*- and *O*-glycans has been associated with *G6PT* mutations in patients with glycogen storage disease type 1b and recurrent bacterial infections and with mutations in *G6PC3* in a subset of patients with severe congenital neutropenia.<sup>11-13</sup> Moreover, mutations in the CDG genes *SLC35C1* (CDG-IIc)<sup>14</sup> and *ALG1* (CDG-Ik)<sup>15</sup> cause immune defects. *SLC35C1* deficiency occurs in a PID termed leukocyte adhesion deficiency type II.<sup>16</sup>

The phosphoglucomutases belong to the family of phosphohexose mutases that catalyze the reversible conversion of glucose-1-phosphate to glucose-6-phosphate. In contrast, the ubiquitously expressed human phosphoglucomutase 3 (PGM3; identical to phosphoacetylglucosamine mutase 1 [AGM1]), catalyzes the conversion of N-acetyl-D-glucosamine-6-phosphate (GlcNAc-6-P) to N-acetyl-D-glucosamine-1-phosphate (GlcNAc-1-P), which is required for the biosynthesis of uridine diphosphate N-acetylglucosamine (UDP-GlcNAc), an essential precursor for protein glycosylation.<sup>17,18</sup> Hence deficiencies in PGM3 are likely to impair glycan-mediated processes, such as cell-cell recognition or immune signaling.

In mice *Pgm3*-mediated UDP-GlcNAc synthesis is essential for hematopoiesis and development, and distinct recessive hypomorphic *Pgm3* mutations lead to overlapping but not identical phenotypes.<sup>19</sup>

In this study we identified mutations in *PGM3/AGM1* in 9 patients from 4 consanguineous families with recurrent infections

and increased serum IgE levels but normal *STAT3* and *DOCK8*. Biallelic hypomorphic *PGM3* mutations were associated with impaired glycosylation caused by impaired PGM3 function and thus characterize a novel group of primary (inborn) immune deficiencies with a hyper-IgE-like syndrome.

## METHODS

### Patients and control subjects

This study was conducted under human subjects' protocols approved by local ethics committees at University College London; the University of Freiburg; the Pasteur Institute of Tunis; Erciyes University, Turkey; and Hassan II University, Morocco. Six patients with HIES with an autosomal recessive (AR) inheritance pattern from 2 Tunisian families (families A and B), 1 patient from a Turkish family (family C), and 2 patients from a Moroccan family (family D) were the focus of this study. A further 30 affected subjects were tested for *PGM3* mutations. One hundred seventy unaffected subjects originating from Tunisia (n = 100), Morocco (n = 20), and Turkey (n = 50) served as control subjects. The race or ethnic group of the Tunisian control subjects was self-reported and considered "North African." Written consent was given by study participants, their parental guardians, or both according to local ethics committee requirements.

Supplemental information on the methods used in this study can be found in the Methods section in this article's Online Repository at [www.jacionline.org](http://www.jacionline.org).

## RESULTS

### Clinical assessments of affected subjects

All patients in this study have received independent diagnoses of HIES based on the clinical triad of recurrent pneumonia,

**TABLE II.** (Continued)

Patients			
A.V.18	B.V.6	B.V.7	C.IV.7
6 y	7 y	6 y	9 y
17,060 ↑ (5,200-11,000)	12,100 ↑ (4,400-9,500)	16,100 ↑ (5,200-11,000)	2,280 ↓ (4,400-9,500)
12,610 ↑ (1,700-7,000)	6,410 (1,700-7,000)	9,660 ↑ (1,700-7,000)	1,090 (1,000-5,000)
2,630 (2,300-5,400)	3,150 (1,900-3,700)	3,500 (2,300-5,400)	760 ↓ (1,900-3,700)
510-1,410 ↑ (160-800)	800-1,500 ↑ (100-600)	1,450-2,000 ↑ (160-800)	900 ↑ (100-800)
606 ↑ (130-400)	600 ↑ (130-400)	670 ↑ (130-400)	199 (130-400)
53 ↓ (56-75)	35 ↓ (60-76)	71 (56-75)	87.9 ↑ (60-76)
14.5 ↓ (28-47)	29 ↓ (31-47)	25 ↓ (28-47)	46.2 (31-47)
41 ↑ (16-30)	42 ↑ (18-35)	42 ↑ (16-30)	41.2 ↑ (18-35)
0.35 (1.57-1.75)	0.69 (1.34-1.72)	0.6 (1.57-1.75)	1.12 (1.34-1.72)
8.5 ↓ (14-33)	20 (13-27)	42 ↑ (14-33)	1 ↓ (13-27)
47 ↑ (3-17)	14 (4-17)	46 ↑ (3-17)	5.5 (4-17)
Lymphocyte subsets (counts/ $\mu$ L)			
1,400 ↓ (1,470-1,970)	1,100 ↓ (2,120-2,680)	2,490 ↓ (1,470-1,970)	670 ↑ (456-580)
381 ↓ (740-1,220)	913 ↓ (1,100-1,700)	875 ↓ (740-1,220)	350 (240-360)
1,080 ↑ (416-790)	1,320 ↑ (635-1,235)	1,470 ↑ (416-790)	313 ↑ (140-266)
224 ↓ (370-870)	630 (460-950)	1,470 ↑ (370-870)	7.6 ↓ (100-205)
1,240 ↑ (80-450)	441 (141-600)	1,610 ↑ (80-450)	42 (23-130)
Serum immunoglobulins			
0.698 (0.4-2)	1.45 (0.75-1.97)	3 ↑ (0.4-2)	0.4 ↓ (0.75-1.97)
9.034 (8-15)	15.6 (5-17)	16 ↑ (8-15)	14.6 (8-19)
0.837 (0.75-2)	3.40 ↑ (0.85-2.2)	2.05 ↑ (0.75-2)	3.8 ↑ (0.85-2.2)
16,534 ↑ (0-200)	99,600 ↑ (0-200)	141,300 ↑ (0-200)	9,320 ↑ (0-200)
Normal	Normal	Normal	Normal

recurrent skin abscesses, and a highly increased serum IgE level. Family B has been previously described as having Buckley syndrome, a synonym for HIES.<sup>20</sup> Clinical and laboratory findings, B- and T-cell phenotyping, and T-cell proliferation are summarized in Tables I to IV<sup>21</sup> and Figs E1 and E2 in this article's Online Repository at [www.jacionline.org](http://www.jacionline.org). In summary, eosinophilia and an inverted CD4/CD8 ratio, in addition to the increase in serum IgE levels, were characteristic laboratory findings in our patients. As known for other CDGs, most routine laboratory values were not consistently altered in all patients. Remarkably, most patients with *PGM3* mutations had developmental delay, and many had psychomotor retardation, resembling clinical findings in patients with CDGs.

### Identification of *PGM3* mutations by using homozygosity mapping/linkage analysis and selector-based sequencing

Using a positional approach to identify the disease-causing mutations in both Tunisian families A and B (Fig 1, A and B), we identified overlapping perfect intervals on chromosome 6q. Family B had a huge perfect interval spanning chr6:54.3-107.0Mbp (build 36/hg18 positions), and family A had its largest perfect interval at chr6:73.2-85.1Mbp. Perfectly segregating intervals in these families yielded logarithm of odds (LOD) scores of at least 3.32 for family A and 1.65 for family B, with a multipoint LOD score of at least 4.97. We thus hypothesized that they might have the same monogenic

disease but, because of the more severe phenotype in family A, not necessarily the same mutation. The intersection of the 2 intervals, chr6:73.2-85.1Mbp, contained 45 candidate genes (see Table E1 in this article's Online Repository at [www.jacionline.org](http://www.jacionline.org)), and both families shared a small disease-associated haplotype at chr6:82.88-83.40Mbp. However, in a candidate approach comprising several genes associated with immune functions, mutations in the coding exons or flanking intronic regions were not detected.

Therefore we performed selector-based,<sup>22</sup> high-throughput sequencing of all coding exons, exon/intron boundaries, and untranslated regions of all 45 genes in the predicted region. We identified 2 sequence variants in *PGM3* (ENSP00000424874/PGM3-001/NP\_056414), which spans 29 kb, comprises 14 exons, and encodes PGM3. Exon 3 contains the start codon for transcript variant 1, which encodes the 542-amino-acid PGM3 isoform 2 (see the Results section in this article's Online Repository at [www.jacionline.org](http://www.jacionline.org)). Both mutations affect highly conserved amino acid residues and predict a 1-amino-acid deletion, p.Glu340del (c.1018\_1020del; exon 9), in family A (Fig 1, E), and a substitution, p.Leu83Ser (c.248T>C; exon 4), in family B (Fig 1, F), respectively. Modeling the p.Leu83Ser mutation *in silico* predicted the most deleterious effect (PolyPhen<sup>23</sup> prediction: probably damaging; SIFT<sup>24</sup> score, 0.00).

We next sequenced *PGM3* in 32 unrelated patients, with phenotypes resembling autosomal dominant (AD) HIES or AR-HIES but without mutations in *STAT3* or *DOCK8*. In the affected patient of a consanguineous Turkish family (family C;

**TABLE III.** B- and T-cell phenotyping

	Patient					Travel control	Reference range
	B.V.6	B.V.7	C.IV.7	D.IV.2	D.IV.5		
CD19 <sup>+</sup> B cells	12.26	28.11 ↑	1.07 ↓	9.04	7.06	18.6	4.9-18.4
CD27 <sup>-</sup> IgD <sup>+</sup> (naive)	62.72	77.08	24.75 ↓	69.6	75.6	54.61	42.6-82.3 (% CD19 <sup>+</sup> )
CD27 <sup>+</sup> IgD <sup>+</sup> (IgM memory)	23.99	4.68 ↓	3.52 ↓	13.12	13.9	9.34	7.4-32.5 (% CD19 <sup>+</sup> )
CD27 <sup>+</sup> IgD <sup>-</sup> (switched memory)	7.70	7.30	52.39 ↑	12.66	5.59 ↓	21.62	6.5-29.1 (% CD19 <sup>+</sup> )
CD27 <sup>+</sup> IgD <sup>-</sup> (switched memory)	0.94	2.05	0.56	1.19	0.43	3.93	0.25-7.0 (% PBL)
CD21 <sup>-</sup> CD38 <sup>-</sup>	8.20 ↑	1.79	11.86 ↑	11.5 ↑	5.29	7.84	0.9-7.6 (% CD19 <sup>+</sup> )
Transitional B cells	2.34	0.81	8.89 ↑	4.92 ↑	7.92 ↑	1.48	0.6-3.4
Plasmablasts	0.05 ↓	0.05 ↓	14.82 ↑	3.45	1.3	0.09 ↓	0.4-3.6
CD3 <sup>+</sup> (total T cells)	78	58	88 ↑	95.7 ↑	91.9 ↑	56	52-83 (% lymphocytes)
CD3 <sup>+</sup> CD4 <sup>+</sup> (CD4 T cells)	26	41	48	ND	ND	24	24-57 (% lymphocytes)
CD3 <sup>+</sup> CD8 <sup>+</sup> (CD8 T cells)	45 ↑	14	32	ND	ND	24	9-39 (% lymphocytes)
CD4 <sup>+</sup> CD45RO <sup>+</sup> (CD4 memory)	90 ↑	90 ↑	95 ↑	ND	ND	56	35-82 (% CD4 <sup>+</sup> )
CD4 <sup>+</sup> CD45RO <sup>+</sup> CXCR5 <sup>+</sup> (TFH)	5	8	2 ↓	ND	ND	2 ↓	4-13 (% CD4 <sup>+</sup> )
CD4 <sup>+</sup> CD45RO <sup>+</sup> CXCR5 <sup>+</sup> (TFH)	6	9	2 ↓	ND	ND	4	4-13 (% memory)
CD8 <sup>+</sup> CD27 <sup>-</sup> CD28 <sup>-</sup> (late effector)	71 ↑	25	84 ↑	48.9 ↑	58.1 ↑	10	2-36 (% CD8 <sup>+</sup> )
CD8 <sup>+</sup> CD27 <sup>+</sup> CD28 <sup>-</sup> (effector)	18 ↑	46 ↑	6	44.5 ↑	37.2 ↑	10	3-17 (% CD8 <sup>+</sup> )
CD4 <sup>-</sup> CD8 <sup>-</sup> (double negative T)	2	1	2	0.9	1.6	4 ↑	0.4-2.2 (% TCRαβ <sup>+</sup> )
CD4 <sup>+</sup> CD45RA <sup>+</sup> (CD4 naive)	12 ↓	11 ↓	2 ↓	ND	ND	31	31-72 (% CD4 <sup>+</sup> )
CD4 <sup>+</sup> CD45RA <sup>+</sup> CD31 <sup>+</sup> (RTEs)	8 ↓	7 ↓	1 ↓	ND	ND	16	12-30 (% CD4 <sup>+</sup> )
CD4 <sup>+</sup> CD45RA <sup>+</sup> CD31 <sup>+</sup> (RTEs)	67	64	35 ↓	53.5	52.9	52	41-79 (% naive)
CD4 <sup>+</sup> CD45RO <sup>+</sup> IFN-γ <sup>+</sup>	22.53	14.17	20.73	ND	ND	15.61	13.8-29 (% CD4 <sup>+</sup> CD45RO <sup>+</sup> )
CD4 <sup>+</sup> CD45RO <sup>+</sup> IL-4 <sup>+</sup>	9.81	18.83 ↑	26.57 ↑	ND	ND	11.10	4-12.1 (% CD4 <sup>+</sup> CD45RO <sup>+</sup> )
CD4 <sup>+</sup> CD25 <sup>hi</sup> FoxP3 <sup>+</sup>	2.22	3.46	1.08 ↓	ND	ND	4.58	1.7-7.8 (% CD4 <sup>+</sup> )
CD4 <sup>+</sup> CD45RO <sup>+</sup> IL-17 <sup>+</sup>	0.72 ↓	1.02 ↓	1.07 ↓	ND	ND	0.79 ↓	1.2-5.1 (% CD4 <sup>+</sup> CD45RO <sup>+</sup> )

Values are shown as percentages.

FoxP3, Forkhead box protein 3; ND, not done; PBL, peripheral blood lymphocytes; RTEs, recent thymic emigrants; TCR, T-cell receptor; TFH, follicular T<sub>H</sub> cells.

**TABLE IV.** Decreased *in vitro* T-cell proliferation in patients with *PGM3* mutations

Patient	PHA	Anti-CD3	PPD	TT
A.V.12	35	29.1	5.6	4.1
A.V.13	30	2.5	1.2	1.9
A.V.14	24	6.4	4.8	1.9
A.V.18	25	12.8	9.6	1.7
B.V.6	186	45.3	2.0	2.3
B.V.7	71	51.4	9.3	1.4
Control (n = 4)	78 ± 52.7	13 ± 6	41 ± 19.7	25 ± 17

PBMCs were cultured in the presence of PHA for 3 days or with anti-CD3 or recall antigens (tuberculin [PPD] or tetanus toxoid) for 5 to 6 days. Values are expressed as stimulation indexes, which were calculated as mean counts per minute of triplicates in stimulated cultures versus control values. For the control values, the SD of the mean is indicated. A stimulation index of less than 2 is considered absent.

PPD, Purified protein derivative; TT, tetanus toxoid.

**Fig 1, C and G**, we identified a third homozygous point mutation in *PGM3* (p.Asp502Tyr; c.1504G>T; exon 13), which is also predicted to be damaging by both PolyPhen and SIFT (score, 0.00). Furthermore, the index patient with HIES from Morocco and an affected sibling (family D; **Fig 1, D and H**) carry the same mutation, p.Leu83Ser (c.248T>C), as identified in family B. Genotype data on family D are not available to evaluate whether families B and D have a common ancestor.

The *PGM3* mutations (see **Table E2** in this article's Online Repository at [www.jacionline.org](http://www.jacionline.org)) segregate perfectly with the disease phenotype in each family (**Fig 1**). The variants were absent in 170 control subjects from Tunisia (n = 100), Turkey (n = 50), and Morocco (n = 20), excluding that the novel mutations are polymorphisms in these populations.

### Impaired PGM3 expression in affected subjects carrying homozygous p.Glu340del mutations

PGM3 comprises 4 functional domains (**Fig 2, A**). The identified mutations are located in the N-terminal catalytic (p.Leu83Ser; families B and D), the central sugar-binding (p.Glu340del; family A), and the C-terminal PO<sub>4</sub><sup>-</sup>-binding (p.Asp502Tyr; family C) domains of the protein, respectively. Thus each of the identified mutations predicts the loss of a unique protein function. To test whether PGM3 expression was impaired, we analyzed lysates from immortalized B or T cells derived from patients and unaffected members from families A, B, and C and from control subjects by means of Western blotting (**Fig 2, B** and **C**). PGM3 was expressed at similar levels in patients B.V.7 (homozygous for p.Leu83Ser) and C.IV.7 (homozygous for p.Asp502Tyr), as well as in all analyzed heterozygous carriers, whereas patients A.V.12 and A.V.18 (both homozygous for p.Glu340del) showed markedly decreased expression. The latter suggest that the homozygous mutation in family A, affecting the sugar-binding domain, not only causes protein dysfunction but probably also leads to increased protein degradation.

### Mutant PGM3 shows reduced catalytic activity but retains its specificity

The assembly of mono-antennary, bi-antennary, tri-antennary, and tetra-antennary branched N-glycans is dependent on the supply of a common substrate UDP-GlcNAc. Because PGM3 catalyzes the bidirectional conversion of GlcNAc-6-P to GlcNAc-1-P, which is required for the synthesis of UDP-GlcNAc, we hypothesized that impaired PGM3 function leads to aberrant N-glycosylation (**Fig 3, A**). However the *PGM3* mutations in our

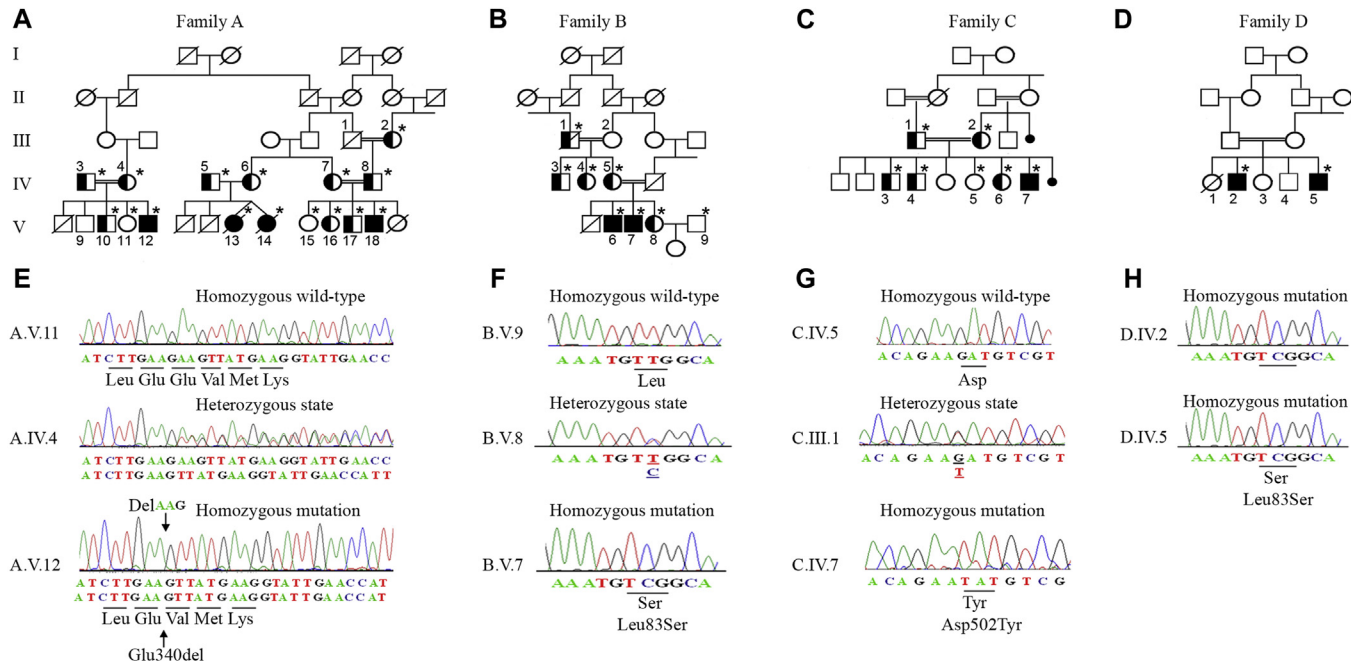


**FIG 1.** Segregation of *PGM3* mutations with disease status in families with AR-HIES. **A-D**, Family A, p.Glu340del; families B and D, p.Leu83Ser; and family C, p.Asp502Tyr. Circles, Female subjects; squares, male subjects; solid symbols, affected subjects; half-solid symbols, heterozygous carriers; open symbols, healthy members with wild-type *PGM3*; slashes, deceased subjects; double horizontal lines, consanguinity; black dots, miscarriages. Asterisks indicate mutations confirmed by using sequencing. **E-H**, Sequence analyses of unaffected subjects without *PGM3* mutations (top), unaffected heterozygous carriers (middle) in Fig 1, E-G), and homozygous affected subjects (bottom).

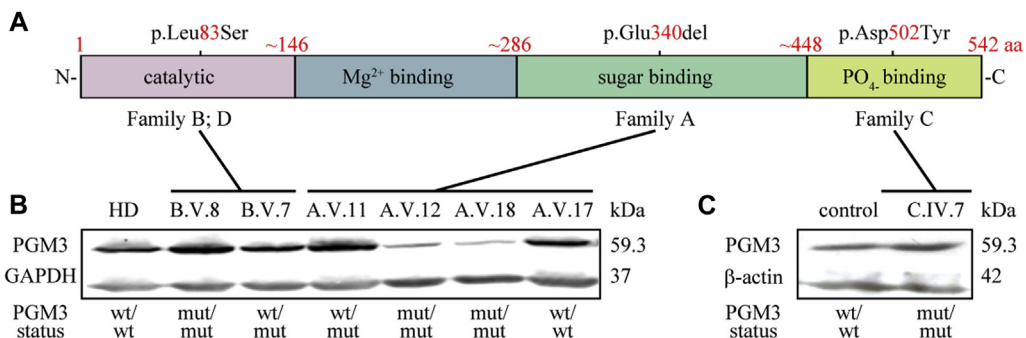


**FIG 2.** Homozygous p.Glu340del mutations within the sugar-binding domain cause reduced PGM3 expression. **A**, Identified mutations localize to distinct protein domains. Numbers indicate amino acid residues. **B**, Western blotting shows reduced PGM3 abundance in EBV-transformed B cells from both homozygous carriers of family A. Mutational status is indicated below each lane. Glyceraldehyde-3-phosphate dehydrogenase (GAPDH) confirms equal loading. HD, Healthy donor. **C**, Normal PGM3 expression in immortalized T cells from the patient in family C who had insufficient B-cell numbers.  $\beta$ -actin was used as a loading control.

patients (A.V.12 and C.IV.7), did not affect the glycosylation pattern of transferrin in the blood (see Fig E3 in this article's Online Repository at [www.jacionline.org](http://www.jacionline.org)), which is a commonly used diagnostic test for congenital defects of glycosylation.<sup>25</sup> Enzymatic testing revealed that the catalytic activity is reduced in mutant PGM3, depending on the substrate dose, with 20% to 30% of residual activity (Fig 3, B). The effect was more pronounced with the p.Glu340del mutation (family A;  $P < .0005$  at 12.5  $\mu$ mol/L GlcNAc-6-P) than with the p.Leu83Ser mutation (family B,  $P < .002$ ). We concluded that the mutant PGM3 retains

its catalytic specificity, although with impaired enzymatic activity. In the accompanying article by Zhang et al,<sup>26</sup> a biochemical defect was shown by analyzing intracellular UDP-GlcNAc levels.

### PGM3 mutations inhibit the formation of complex N-glycan subtypes

By using a common substrate (UDP-GlcNAc), the GlcNAc transferases I (Michaelis-Menten constant Km 0.04) and II

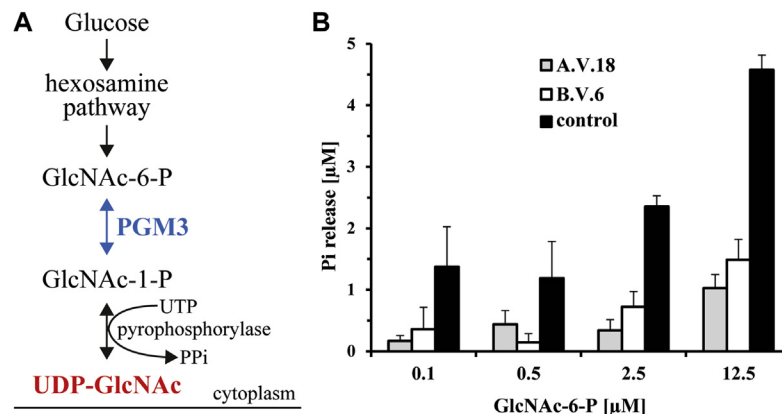


**FIG 3.** Impaired enzymatic activity in mutant PGM3. **A,** PGM3 (blue) catalyzes the change from GlcNAc-6-P to GlcNAc-1-P, which is required for synthesis of UDP-GlcNAc (red). UDP-GlcNAc is the common substrate for assembly of N-glycans. *PPi*, Inorganic pyrophosphate; *UTP*, uridine triphosphate. **B,** Significantly decreased production of inorganic phosphate in EBV-B cell lysates derived from patients A.V.18 (p.Glu340-del;  $P < .0005$  at 12.5  $\mu\text{mol/L}$ ) is more pronounced than that from patient B.V.6 (p.Leu83Ser;  $P < .002$  at 12.5  $\mu\text{mol/L}$ ). Compared with the control ( $n = 2$ ), residual substrate-dependent activity (20% to 30%) of PGM3 is observed. Data were calculated from 3 independent experiments, and SDs are indicated by error bars. *P* values were calculated by using the Student *t* test.

( $K_m$  0.96) initiate the first and second N-glycan antennae, whereas transferases IV ( $K_m$  5.0) and V ( $K_m$  11.0) are required for the third and fourth N-glycan antennae, respectively (Fig 4, A).<sup>27</sup> Because of the higher  $K_m$  value (which in Michaelis-Menten kinetics corresponds to low substrate affinity and thus a low catalytic activity), the initiation of the third and fourth antennae by GlcNAc transferase IV and GlcNAc transferase V requires higher substrate concentrations and will be most impaired if the level of the common substrate is aberrantly low.<sup>27</sup>

Because PGM3 is involved in the production of UDP-GlcNAc and mutations in PGM3 therefore might alter the N-glycomes in affected patients, we performed glycomic profiling of neutrophils from patients B.V.7 (p.Leu83Ser) and C.IV.7 (p.Asp502Tyr). In both patients we observed decreased levels of tri-antennary and tetra-antennary N-glycans compared with those seen in control subjects (Fig 4, B,<sup>28</sup> and see Fig E4 in this article's Online Repository at [www.jacionline.org](http://www.jacionline.org)). Simultaneously, in patient B.V.7 and, to a lesser extent, in patient C.IV.7, bi-antennary N-glycan types accumulated. We also examined EBV-transformed B cells from patients A.V.13 (p.Glu340del) and B.V.7 (p.Leu83Ser) and observed a similar reduction in complex-type tri-antennary and tetra-antennary glycans (Fig 4, C; and see Fig E5 in this article's Online Repository at [www.jacionline.org](http://www.jacionline.org)). The patient from family A showed a substantial accumulation of the hybrid glycans, whereas levels of the bi-antennary, tri-antennary, and tetra-antennary glycans were accordingly decreased. Thus the p.Glu340del mutation in family A predominantly blocks the formation of bi-antennary N-glycans. In contrast, in patient B.V.7 only tri-antennary and tetra-antennary glycan levels were reduced. Thus because glycosylation appears to be retarded at the bi-antennary stage, normal levels of hybrid glycans were observed, which is consistent with the suggested lower severity of the mutation (p.Leu83Ser).

In summary, the homozygous mutation in the sugar-binding domain (p.Glu340del in family A) leads to reduced PGM3 abundance and impairs PGM3 function and glycosylation to a

higher extent than mutations in the catalytic or phosphate-binding domain, respectively, and, as a consequence, causes a more severe clinical phenotype.

Increased serum IgE levels in patients with *PGM3* mutations might be caused by increased IgE stability caused by aberrant glycosylation.<sup>29</sup> However, no significant differences were observed when IgE N-glycan profiles from a patient with *PGM3* mutations and a patient with atopic dermatitis were compared (see Fig E6 in this article's Online Repository at [www.jacionline.org](http://www.jacionline.org)).

### Normal chemotaxis and surface expression of glycosylphosphatidylinositol-anchored proteins on granulocytes

To test whether the *PGM3* mutations influence the expression of surface molecules, which are strongly dependent on the presence of membrane anchors (glycosylphosphatidylinositol [GPI]-anchored proteins), we analyzed the expression of CD59, CD55 (DAF), CD24, CD14, and fluorescently labeled aerolysin binding tightly and specifically to mammalian GPI anchors (FLAER) on granulocytes from patients B.V.6 and B.V.7 by using flow cytometry (see Fig E7 in this article's Online Repository at [www.jacionline.org](http://www.jacionline.org)). However, we could not demonstrate that the p.Leu83Ser mutation alters the expression of the candidate surface proteins because of defective glycosylation of their membrane anchors.

To test whether the impaired glycosylation affects neutrophil function, we analyzed neutrophil chemotaxis in 2 Tunisian patients from family B and the Turkish patient after staining with Calcein-AM and stimulation with N-formyl-methionyl-leucyl-phenylalanine, platelet-activating factor, and C5a, by using a transwell assay. However, when measuring fluorescence intensities on a PerkinElmer EnVision reader (PerkinElmer, Waltham, Mass), we did not find evidence that chemotaxis is altered in patients compared with travel controls (control samples shipped together with the case samples to avoid batch effects, data not shown).

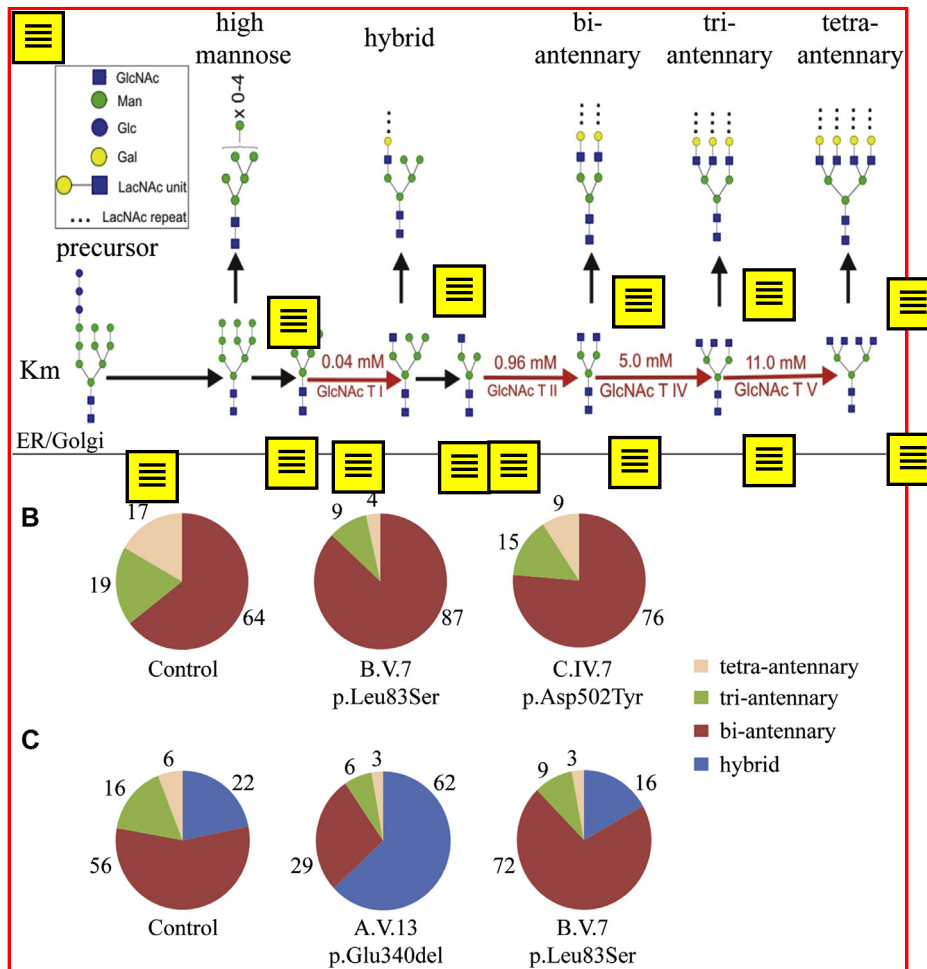


**FIG 4.** Incomplete assembly of complex-type glycans in patients with *PGM3* mutations. **A**, *PGM3* links to N-glycosylation through UDP-GlcNAc (red). The common substrate for assembly of the complex-type N-glycans in the Golgi apparatus (vertical arrows) is used by 4 GlcNAc transferases (transferase [T] I, II, IV, and V; red arrows) with decreasing catalytic activity (increasing Km values [mmol/L UDP-GlcNAc]).<sup>27</sup> UDP-GlcNAc produced by mutant *PGM3* might be insufficient to allow for completion of N-glycan antenna formation. *ER*, Endoplasmic reticulum. **B**, Accumulation of bi-antennary N-glycans in neutrophils<sup>28</sup> from patients with *PGM3* mutations. Decreased relative abundance of tri-antennary and tetra-antennary glycans (percentage values of N-glycans detected by using glycomic profiling; see Figs E4 and E5) in affected patients B.V.7 (p.Leu83Ser; catalytic domain) and to a lesser extent in affected patient C.IV.7 (p.Asp502Tyr; phosphate-binding domain). **C**, The homozygous *PGM3* mutation p.Glu340del causes accumulation of the hybrid-type N-glycans, with a simultaneous decrease in bi-antennary, tri-antennary, and tetra-antennary N-glycan levels in EBV B cells from patient A.V.13 (p.Glu340del; sugar-binding domain). B cells from patient B.V.7 (p.Leu83Ser; catalytic domain) have decreased tri-antennary and tetra-antennary N-glycan levels and increased bi-antennary N-glycan levels. Percentage values indicate the relative abundance of glycan types.

### Impaired T-cell proliferation, T<sub>H</sub>2 skewing, and borderline T<sub>H</sub>17 cell numbers in patients with *PGM3* mutations

To test whether the HIES phenotype in our patients with *PGM3* mutations is associated with impaired T-cell function, we analyzed freshly isolated PBMCs using fluorescence-activated cell sorting (FACS) analysis for proliferation and T cell-specific cytokine responses after stimulation *ex vivo* (Tables III and IV and see Figs E1 and E2; see also the accompanying article by Zhang et al<sup>26</sup>). T-cell proliferation to recall antigens (purified protein derivative of tuberculin and tetanus toxoid) was reduced in all samples tested (Table IV). Interestingly, T-cell proliferation after stimulation with PHA or anti-CD3 of family B carrying the missense mutation (p.Leu83Ser) was comparable with that seen

in healthy control subjects; however, proliferation in family A, with the more severe mutation (p.Glu340del), was again borderline low.

The serum IgE level increase might be explained by abnormal T<sub>H</sub> cell differentiation. Therefore we analyzed T<sub>H</sub>1-T<sub>H</sub>2 subsets in our patients by using intracellular IL-4 and IFN- $\gamma$  staining (Table III and see Fig E1). Two of 4 patients tested had grossly increased percentages of T<sub>H</sub>2 cells (19% and 27%, respectively), likely contributing to the increased serum IgE levels seen in these patients.

In contrast to the other patients, B cells were absent in patient C.IV.7, and an unusual subpopulation of CD4 $^{+}$  cells was detected, simultaneously expressing T<sub>H</sub>1 and T<sub>H</sub>2 cytokines, as well as a reduced proportion of forkhead box protein 3-expressing regulatory T cells (data not shown).

STAT3-deficient HIES is characterized by the absence of T<sub>H</sub>17 cells.<sup>30</sup> In our patients with *PGM3* mutations, we found borderline low T<sub>H</sub>17 cell numbers (Table III), with a lower IL-17 phorbol 12-myristate 13-acetate (PMA)/ionomycin stimulation index when compared with that seen in healthy family members. This observation might contribute to the increased infection susceptibility of the skin and mucous membranes in patients with *PGM3* mutations.

## DISCUSSION

We report on homozygous mutations in *PGM3* leading to aberrant glycosylation patterns in leukocytes. Mutations in *PGM3* have previously not been associated with human disease. Here we demonstrate that hypomorphic mutations in *PGM3* constitute a novel genetic defect in patients previously given a diagnosis of AR-HIES.

*PGM3* has previously been shown to contain a polymorphism with a high minor allele frequency, which is useful for population genetic studies.<sup>31</sup> The mutations described herein, including 2 nonsynonymous point mutations and a single codon deletion in 9 patients from 4 unrelated families, respectively, have not been identified in other ethnic groups and are not listed in the Human Gene Mutation Database or the 1000 Genomes project. They affect all 4 known *PGM3* isoforms and localize to 3 of the 4 functional protein domains, thus predicting the loss of distinct protein functions.

All patients in our study were given independent diagnoses of HIES in 3 clinical immunology centers solely on the basis of their clinical presentation, including increased serum IgE levels, recurrent skin and pulmonary infections, abscesses, eczema, and bronchiectasis. In a previous study,<sup>20</sup> 2 patients (B.V.6 and B.V.7) were reported as having Buckley syndrome, which is an alternative name for HIES. Criteria to distinguish patients with biallelic *PGM3* mutations from other patients with HIES might be a reversed CD4/CD8 ratio and developmental delay.

AR-HIES often occurs in consanguineous families, and approximately 80% of affected subjects carry a mutation in *DOCK8* (Engelhardt et al, manuscript in preparation). Although the clinical presentations are similar, only one of the 9 patients with *PGM3* mutations had severe chicken pox, and none had a food allergy; in contrast, severe cutaneous viral infections and food allergies occur in 70% of cases of *DOCK8* deficiency.<sup>6,7</sup> In addition, failure to thrive is more prevalent in subjects with mutations in *PGM3* (89%) than in subjects with mutations in *DOCK8* (58%) and frequently coincided with developmental delay and psychomotor retardation, which is reminiscent of CDG but not of *DOCK8* deficiency. Phenotypic discrimination between patients with HIES with *STAT3* or with *PGM3* mutations is less apparent and includes pneumatoceles and dental abnormalities, which occur in patients with *STAT3*-associated AD-HIES<sup>5</sup> but not in affected patients with *PGM3* mutations. However, connective tissue and skeletal abnormalities, joint hyperextensibility, scoliosis, and a characteristic face occur in both. Thus our results indicate that *PGM3* deficiency is a CDG characterizing a novel subtype of AR-HIES.

In family A the p.Glu340del mutation not only led to the most severe pathology and reduced *PGM3* abundance but also blocked the formation of bi-antennary N-glycans. In contrast, in families B (p.Leu83Ser) and C (p.Asp502Tyr) the bi-antennary

N-glycans accumulated, and the neurologic disorders were milder. This observation is consistent with a genotype-phenotype correlation. In support of this view, the accompanying article by Zhang et al<sup>26</sup> describes additional patients with HIES from 2 families carrying distinct *PGM3* mutations. All patients presented with bronchiectasis, eczema, abscesses, and developmental delays, as observed in our cohort. However, their patients have CD8 lymphopenia, high cholesterol levels, and renal and liver changes that are not present in our patients with *PGM3* mutations.

It has been reported that *Pgm3* deficiency causes embryonic lethality in mice,<sup>19</sup> whereas *Pgm3* gene-trap mice showed reduced body weight, defective B-lymphocyte development, and neurodegeneration caused by decreased UDP-GlcNAc levels in the brain. Accordingly, in the majority of patients with *PGM3* mutations, we observed failure to thrive, decreased B-cell numbers, and, in some patients, developmental delay. In contrast, increased numbers of platelets and eosinophilic granulocytes and a reverted CD4/CD8 ratio were not observed in *Pgm3* mutant mice.

In patients with congenital disorder of glycosylation type II (OMIM no. 212066), mutations in *MGAT2* (encoding GlcNAc T II which operates downstream of *PGM3*) cause severe multisystemic developmental anomalies and reduced abundance of bi-antennary, tri-antennary, and tetra-antennary glycans.<sup>32-34</sup> The similarities to patients with *PGM3* mutations indicate that complex N-glycans are essential for normal neuronal development. In patients with congenital dyserythropoietic anemia type II (OMIM no. 224100), glycomics analysis of erythrocytes showed increased levels of immature hybrid glycans and a marked reduction in branched mature glycan levels,<sup>35</sup> as we observed in the leukocytes of our patients.

Because we did not find convincing evidence for defective N-glycosylation or decreased turnover of IgE, the exact cause for increased serum IgE levels in patients with *PGM3* mutations, as for other forms of HIES, remains to be determined, although we have demonstrated an abnormal T<sub>H</sub>1/T<sub>H</sub>2 differentiation in 2 of 4 patients tested. Therefore we have to conclude that the pathogenic mechanism of how the aberrant glycosylation leads to the observed HIES-like phenotype remains elusive.

However, the observation that inheritable defects of glycosylation can lead to an HIES-like phenotype has not been recognized previously.<sup>36-38</sup> Although mutations in *PGM1* can cause a CDG-like phenotype, neurologic or immunologic disorders, as in our patients with *PGM3* mutations, were not earlier observed.<sup>39</sup> Certainly, in addition to defective glycan biosynthesis, other pathogenic mechanisms, such as abrogated membrane transport or gain-of-glycosylation sites, can also account for immune deficiencies.<sup>40,41</sup> Whether hematopoietic stem cell transplantation, a successful treatment option in patients with *DOCK8* deficiency,<sup>42</sup> is also effective for patients with *PGM3* mutations has not yet been confirmed.

Our observation that congenital glycosylation defects can be associated with a rare HIES-like PID raises the possibility that the prevalent IgE-mediated allergy and atopy seen in these patients might also, at least in part, be due to aberrant glycosylation.

We thank Dr Steven Holland (National Institutes of Health) for initial screening of Tunisian affected subjects for *STAT3* mutations, Dr Khaled Ayed for useful discussions, Nabil Belhaj Hmida for field work, Beya Largueche for technical assistance, Dr Yadhu Kumar and Dr Malkanthi Fernando for transferrin analysis, Monika Häffner for performing neutrophil chemotaxis

assays, and Dr Christopher Bauser, GATC Biotech AG, Konstanz, Germany, for high-throughput sequencing. We are deeply grateful to affected persons and their families for collaboration. This work has first been presented at the Joint Meeting of the Society for Glycobiology & American Society for Matrix Biology, November 11-14, 2012, San Diego, California.

**Clinical implications: Hypomorphic mutations in *PGM3* are associated with defects in immunity and development in a novel form of PID with impaired cell- and tissue-specific glycosylation.**

**REFERENCES**

1. Notarangelo LD. Primary immunodeficiencies. *J Allergy Clin Immunol* 2010;125:182-94.
2. Casanova J-L, Abel L. Primary Immunodeficiencies: a field in its infancy. *Science* 2007;317:617-9.
3. Marodi L, Notarangelo LD. Immunological and genetic basis of primary immunodeficiencies. *Nat Rev Immunol* 2007;7:851-61.
4. Holland SM, DeLeo FR, Elloumi HZ, Hsu AP, Uzel G, Brodsky N, et al. *STAT3* mutations in the hyper-IgE syndrome. *N Engl J Med* 2007;357:1608-19.
5. Woellner C, Gertz EM, Schäffer AA, Lagos M, Perro M, Glocker E-O, et al. Mutations in *STAT3* and diagnostic guidelines for hyper-IgE syndrome. *J Allergy Clin Immunol* 2010;125:424-32.
6. Zhang Q, Davis JC, Lamborn IT, Freeman AF, Jing H, Favreau AJ, et al. Combined immunodeficiency associated with *DOCK8* mutations. *N Engl J Med* 2009;361:2046-55.
7. Engelhardt KR, McGhee S, Winkler S, Sassi A, Woellner C, Lopez-Herrera G, et al. Large deletions and point mutations involving the dedicator of cytokinesis 8 (*DOCK8*) in the autosomal-recessive form of hyper-IgE syndrome. *J Allergy Clin Immunol* 2009;124:1289-302.
8. Minegishi Y, Saito M, Morio T, Watanabe K, Agematsu K, Tsuchiya S, et al. Human tyrosine kinase 2 deficiency reveals its requisite roles in multiple cytokine signals involved in innate and acquired immunity. *Immunity* 2006;25:745-55.
9. Rabinovich GA, van Kooyk I, Cobb BA. Glycobiology of immune responses. *Ann N Y Acad Sci* 2012;1253:1-15.
10. Arnold JN, Wormald MR, Sim RB, Rudd PM, Dwek RA. The impact of glycosylation on the biological function and structure of human immunoglobulins. *Ann Rev Immunol* 2007;25:21-50.
11. Chou JY. The molecular basis of type 1 glycogen storage diseases. *Curr Mol Med* 2001;1:25-44.
12. Bozta K, Appaswamy G, Ashikov A, Schäffer AA, Salzer U, Diestelhorst J, et al. A syndrome with congenital neutropenia and mutations in *G6PC3*. *N Engl J Med* 2009;360:32-43.
13. Hayee B, Antonopoulos A, Murphy EJ, Rahman FZ, Sewell G, Smith BN, et al. *G6PC3* mutations are associated with a major defect of glycosylation: a novel mechanism for neutrophil dysfunction. *Glycobiology* 2011;21:914-24.
14. Gazit Y, Mory A, Etzioni A, Frydman M, Scheuerman O, Gershoni-Baruch R, et al. Leukocyte adhesion deficiency type II: long-term follow-up and review of the literature. *J Clin Immunol* 2010;30:308-13.
15. Grubemann CE, Frank CG, Hülsmeier AJ, Schollen E, Matthijs G, Mayatepek E, et al. Deficiency of the first mannosylation step in the N-glycosylation pathway causes congenital disorder of glycosylation type Ik. *Hum Mol Genet* 2004;13:535-42.
16. Etzioni A, Sturla L, Antonellis A, Green ED, Gershoni-Baruch R, Berninson PM, et al. Leukocyte adhesion deficiency (LAD) type II/carbohydrate deficient glycoprotein (CDG) IIc founder effect and genotype/phenotype correlation. *Am J Med Genet* 2002;110:131-5.
17. Li C, Rodriguez M, Banerjee D. Cloning and characterization of complementary DNA encoding human N-acetylglucosamine-phosphate mutase protein. *Gene* 2000;242:97-103.
18. Pang H, Koda Y, Soejima M, Kimura H. Identification of human PGM3 as N-acetylglucosamine-phosphate mutase (AGM1). *Ann Hum Genet* 2002;66:139-44.
19. Greig KT, Antonchuk J, Metcalf D, Morgan PO, Krebs DL, Zhang J-G, et al. Agm1/Pgm3-mediated sugar nucleotide synthesis is essential for hematopoiesis and development. *Mol Cell Biol* 2007;27:5849-59.
20. Ayed K, Ben Dridi MF, Gorgi Y, Bardi R, Hamzaoui K, Dali S. Forme familiale du syndrome de Buckley avec anomalies de l'immunité cellulaire [Familial form of the Buckley syndrome with anomalies of cellular immunity]. *Ann Pediatr* 1987;34:645-8.
21. Shearer WT, Rosenblatt HM, Gelman RS, Oyomopito R, Plaege S, Stiehm ER, et al. Lymphocyte subsets in healthy children from birth through 18 years of age: the Pediatric AIDS Clinical Trials Group P1009 study. *J Allergy Clin Immunol* 2003;112:973-80.
22. Johansson H, Isaksson M, Falk-Sörqvist E, Roos F, Stenberg J, Sjöblom T, et al. Targeted resequencing of candidate genes using selector probes. *Nucleic Acids Res* 2011;39:e8.
23. Ramensky V, Bork P, Sunyaev S. Human non-synonymous SNPs: server and survey. *Nucleic Acids Res* 2002;30:3894-900.
24. Ng PC, Henikoff S. Accounting for human polymorphisms predicted to affect protein function. *Genome Res* 2002;12:436-46.
25. Babovic-Vuksanovic D, O'Brien JF. Laboratory diagnosis of congenital disorders of glycosylation type I by analysis of transferrin glycoforms. *Mol Diagn Ther* 2007;11:303-11.
26. Zhang Y, Yu X, Ichikawa M, Lyons JJ, Datta S, Lamborn IT, et al. Autosomal recessive phosphoglucomutase 3 (*PGM3*) mutations link glycosylation defects to atopy, immune deficiency, autoimmunity, and neurocognitive impairment. *J Allergy Clin Immunol* 2014 doi:10.1016/j.jaci.2014.02.013.
27. Dennis JW, Nabi IR, Demetriou M. Metabolism, cell surface organization, and disease. *Cell* 2009;139:1229-41.
28. Babu P, North SJ, Jang-Lee J, Chalabi S, Mackerness K, Stowell SR, et al. Structural characterization of neutrophil glycans by ultra sensitive mass spectrometric glycomics methodology. *Glycoconj J* 2009;26:975-86.
29. Ha S, Ou Y, Vlasak J, Li Y, Wang S, Vo K, et al. Isolation and characterization of IgG1 with asymmetrical Fc glycosylation. *Glycobiology* 2011;21:1087-96.
30. Milner JD, Brenchley JM, Laurence A, Freeman AF, Hill BJ, Elias KM, et al. Impaired Th17 cell differentiation in subjects with autosomal dominant hyper-IgE syndrome. *Nature* 2008;452:773-6.
31. Hopkinson DA, Harris H. A third phosphoglucomutase locus in man. *Ann Hum Genet* 1968;31:359-67.
32. Jaeken J, Schachter H, Carchon H, De Cock P, Coddeville B, Spik G. Carbohydrate deficient glycoprotein syndrome type II: a deficiency in Golgi localised N-acetyl-glucosaminyltransferase II. *Arch Dis Child* 1994;71:123-7.
33. Cormier-Daire V, Amiel J, Vuillaumier-Barrot S, Tan J, Durand G, Munnoch A, et al. Congenital disorders of glycosylation IIa cause growth retardation, mental retardation and facial dysmorphisms. *J Med Genet* 2000;37:875.
34. Wang Y, Tan J, Sutton-Smith M, Ditto D, Panico M, Campbell RM, et al. Modeling human congenital disorder of glycosylation type IIa in the mouse: conservation of asparagine-linked glycan-dependent functions in mammalian physiology and insights into disease pathogenesis. *Glycobiology* 2001;11:1051-70.
35. Fukuda MN, Gaetani GF, Izzo P, Scartezzini P, Dell A. Incompletely processed N-glycans of serum glycoproteins in congenital dyserythropoietic anemia type II (HEMPAS). *Br J Haematol* 1992;82:745-52.
36. Jaeken J, Matthijs G. Congenital disorders of glycosylation: a rapidly expanding disease family. *Annu Rev Genomics Hum Genet* 2007;8:261-78.
37. Jaeken J, Hennet T, Matthijs G, Freeze HH. CDG nomenclature: time for a change! *Biochim Biophys Acta* 2009;1792:825-6.
38. Schachter H, Freeze HH. Glycosylation diseases: quo vadis? *Biochim Biophys Acta* 2009;1792:925-30.
39. Pérez B, Medrano C, Ecay MJ, Ruiz-Sala P, Martínez-Pardo M, Ugarte M, et al. A novel congenital disorder of glycosylation type without central nervous system involvement caused by mutations in the phosphoglucomutase 1 gene. *J Inher Metab Dis* 2013;36:535-42.
40. Lünn K, Wild MK, Eckhardt M, Gerardy-Schahn R, Vestweber D. The gene defective in leukocyte adhesion deficiency II encodes a putative GDP-fucose transporter. *Nat Genet* 2001;28:69-72.
41. Vogt G, Chapgier A, Yang K, Chuzhanova N, Feinberg J, Fieschi C, et al. Gains of glycosylation comprise an unexpectedly large group of pathogenic mutations. *Nat Genet* 2005;37:692-700.
42. Metin A, Tavil B, Azkur D, Ok-Bozkaya I, Kocabas C, et al. Successful bone marrow transplantation for DOCK8 deficient hyper IgE syndrome. *Pediatr Transplant* 2012;16:398-9.

## METHODS

### Homozygosity mapping and genetic linkage analysis

Genotyping was done with the Affymetrix (Santa Clara, Calif) Human Mapping 250K Nsp Array, and genotypes were called by using previously described methods.<sup>E1</sup> Initially, 21 subjects from 2 families (family A, 13 samples; family B, 8 samples) with phenotypes resembling AR-HIES were included in the study. We used the software findhomoz<sup>E1</sup> to identify perfect intervals in which the affected subjects were homozygous for an interval of at least 500 kb and the unaffected subjects had a different genotype. UNIX shell scripts were used to compare perfect intervals across the 2 families, but we did not require the disease-associated haplotypes in families A and B to be identical. LOD scores for individual families were computed with FASTLINK version 4.1P,<sup>E2-E4</sup> assuming complete penetrance and a rare disease allele.

### Targeted sequence-capture and high-throughput sequencing

By using an in-house software suite based on the operating principles of PieceMaker<sup>E5</sup> and Disperse,<sup>E6</sup> a selector assay<sup>E7</sup> was designed to cover all exons and flanking intronic sequences ( $\pm 25$  bp) to include splice sites of the 45 genes in the candidate region derived from genetic linkage analysis. The probes were selected with ProbeMaker software.<sup>E8</sup> A subset of 3339 fragments and corresponding selector probes were selected based on fragment length (100–600 nt) and guanosine-cytosine content (20% to 70%) and based on aiming at double-probe redundancy over targeted regions while avoiding repetitive genomic elements in the ends. The design achieved 96.3% coverage of the targeted bases, and the missing bases were found to be in or near repetitive elements. The selector probes and target enrichment kit were obtained from Halo Genomics (Uppsala, Sweden), and selection experiments were performed according to the corresponding protocol.

All samples were analyzed by using MosaikAligner version 1.0.138821 with the parameters -hs 15 -mm 12 -act 20 -mhp 100 -ms 6, allowing for 12 mismatches in a 100-bp read. For aligning to the reference genome (hg18, March 2006 assembly), the JUMP database option was used. With the in-house software, the aligned reads were transposed to genomic positions, and for each position, the number of reads per base was listed. For each insertion and deletion, the number of reads covered was listed separately. From the lists, only positions with at least 10 $\times$  in read depth were considered. Furthermore, the lists were restricted to changes in coding regions and annotated by using SIFT.<sup>E9</sup> Only positions that were homozygous and nonreference in patients and heterozygous in the healthy obligate carrier parents in the respective family were considered to find possible disease-related changes. Specificity was calculated as the proportion of reads mapped uniquely to the genome that mapped to the targeted region.

### Proliferation assays

PBMCs ( $2 \times 10^5$  cells/well in 200  $\mu$ L of medium) were plated in triplicate in microtiter plates (Nunc, Thermo Fisher Scientific, Loughborough, United Kingdom) and stimulated for 3 days with PHA (5  $\mu$ g/mL) or for 5 to 6 days with anti-CD3 antibodies (2.5  $\mu$ g/mL), tuberculin-purified protein derivative (20  $\mu$ g/mL), or tetanus toxin (10  $\mu$ g/mL), respectively, at 37°C/5% CO<sub>2</sub>. Cells were pulsed for 6 hours with 1  $\mu$ Ci/well tritiated thymidine (GE Healthcare, Little Chalfont, United Kingdom), and incorporated radioactivity was counted in a liquid scintillation counter.

### Flow cytometric analysis and cytokine assays

Standard flow cytometric methods were used for staining of cell-surface markers. PBMCs freshly isolated from patients and healthy control subjects were stained with antibodies labeled as follows: CD3-fluorescein isothiocyanate (FITC), CD4-FITC, CD8-FITC, CD19-FITC, and NK (CD16, CD56)-phycoerythrin; all from Becton Dickinson, Franklin Lakes, NJ). Five thousand events for each staining were analyzed on a FACS Vantage cytofluorograph (BD Biosciences) using LYSIS II software. Cytokine and diagnostic assays for surface markers on unstimulated and PMA/ionomycin-stimulated PBMCs were conducted by the Advanced Diagnostics Unit of the

CCI, Freiburg, Germany, with labeled antibodies (BD Biosciences), as indicated (Figs E1 and E2).

### PGM3 transcripts, PCR, and Sanger sequencing

Consistent entries in Ensembl and Entrez propose that *PGM3* spans 29 kb, comprises 14 exons (first exon is noncoding), and has 4 transcript variants and 4 protein isoforms (with disagreement for the shortest isoform). For the description of the identified *PGM3* mutations, we refer to the first transcript variant (ENST00000513973/ENSP00000424874/PGM3-001), which corresponds to isoform 2 and encodes a 542-amino-acid protein (Entrez IDs NM\_015599/NP\_056414). For mutational analysis, we also considered the transcript ENST00000506587/ENSP0000425809/PGM3-002 (NM\_001199917/NP\_001186846), which encodes a 570-amino-acid protein with an N-terminal extension of 28 amino acids (isoform 1). The third transcript, ENST00000512866/ENSP00000421565/PGM3-004 (NM\_00119919/NP\_001186848), encodes the 566-amino-acid isoform 4, which differs from the 542-amino-acid isoform 1 by an extra segment at the C-terminus. The extra segment was not included in the sequence analyses because it apparently has no role in PGM3 enzymatic activity. The shortest isoform, isoform 3, lacks a segment at the N-terminus but has no additional amino acids.

Genomic DNA from patients, relatives, and healthy adult donors was extracted from whole blood by means of phenol/chloroform extraction. Coding genomic regions of *PGM3* (isoforms PGM3-001 and PGM3-002) and their flanking intronic sequences were amplified from genomic DNA by using a standard PCR protocol. Primer sequences are available on request. PCR products were confirmed by means of agarose gel electrophoresis, purified with shrimp alkaline phosphatase (Promega, Southampton, United Kingdom) and exonuclease I (Thermo Scientific, Loughborough, United Kingdom), and sequenced with the ABI PRISM BigDye Terminator Ready Reaction Kit V3.1 (Applied Biosystems, Foster City, Calif) by using the PCR primers as sequencing primers. The sequencing was performed on a 3130xl Applied Biosystems Genetic Analyzer, and data were analyzed with DNA Sequencing Analysis software (version 5.2, Applied Biosystems) and Sequencher (version 4.8; Gene Codes Corp, Ann Arbor, Mich). Exons 4 and 9 of *PGM3* were sequenced in 100 unaffected Tunisian donors, exon 4 was sequenced in an additional 20 Moroccan donors, and exon 13 was sequenced in 50 unaffected Turkish donors to exclude that the identified sequence variations were polymorphisms in these populations.

### Western blotting

*PGM3* protein levels were analyzed in lysates from EBV-transformed B cells derived from a healthy donor (unrelated to both Tunisian families), 2 patients from family A (A.V.12 and A.V.18), 1 patient from family B (B.V.7), unaffected family members heterozygous for a mutation (A.V.17 and B.V.8), and 1 unaffected subject (homozygous wild-type for both mutations [A.V.11]). Alternatively, a herpesvirus saimiri-transformed T-cell line from the patient from family C and 1 unrelated DOCK8-deficient subject (*PGM3*-WT) was analyzed. Glyceraldehyde-3-phosphate dehydrogenase and  $\beta$ -actin were used as loading controls. Samples were separated on 10% SDS-PAGE gels and transferred onto nitrocellulose membranes. Membranes were probed with polyclonal rabbit anti-*PGM3* (Sigma-Aldrich, Dorset, United Kingdom), anti-glyceraldehyde-3-phosphate dehydrogenase (R&D Systems, Abingdon, United Kingdom), and anti- $\beta$ -actin (Novus Biologicals, Cambridge, United Kingdom) antibodies, respectively. Signals were detected with horseradish peroxidase-conjugated goat anti-rabbit IgG antibodies (Cell Signaling, Danvers, Mass) and enhanced chemiluminescence (GE Healthcare, Bucks, United Kingdom).

### Glycomic experiments

Glycomic analysis was performed, as previously described.<sup>E10</sup> Briefly, samples were reduced by using dithiothreitol (Sigma), carboxymethylated by using iodoacetic acid (Sigma), and digested with trypsin (Sigma). N-glycans were released from glycopeptides by using PNGase F (Roche Applied Science, Burgess Hill, United Kingdom), isolated by Sep-Pak C18 cartridge (Waters, Elstree, United Kingdom), permethylated, and purified again with a Sep-Pak C18 cartridge. Matrix-assisted laser desorption/ionization time-of-flight

mass spectrometric analysis was carried out with a Voyager mass spectrometer (Applied Biosystems, Grand Island, NY). All molecular ions are  $[M^+Na]^+$ . Putative structures are based on composition, tandem mass spectrometry, and biosynthetic knowledge. Data were analyzed with Data Explorer (Applied Biosystems) and Glycoworkbench.<sup>E10</sup>

## Determination of PGM3-dependent production of UDP-GlcNAc from GlcNAc-6-P

Enzyme activity was measured with a high-flux assay.<sup>E11</sup> Reactions were carried out in a 100- $\mu$ L volume containing 50 mmol/L Tris-HCl (pH 8.3), 5 mmol/L MgCl<sub>2</sub>, 10% (vol/vol) glycerol, 20  $\mu$ mol/L UTP, GlcNAc-6-P (0.1, 0.5, 2.5 and 12.5  $\mu$ mol/L), 0.5 U/mL pyrophosphatase, 0.1  $\mu$ g of human UDP-N-acetylglucosamine pyrophosphorylase (Abnova, Taipei, Taiwan), and 50  $\mu$ g of lysate from EBV B-cell lines. Samples were incubated at 30°C for 30 minutes and developed with the Malachite Green phosphate assay (ScienCell, Carlsbad, Calif). PGM3 converts GlcNAc-6-P to GlcNAc-1-P, which is processed to UDP-GlcNAc and pyrophosphate by the pyrophosphorylase (Fig 3). Inorganic phosphate (Pi) derived by the pyrophosphatase from the pyrophosphate (PPi) corresponds to PGM3 activity and was quantified by measuring absorbance at 620 nm. Values (in micromoles per liter of Pi) were interpolated from standard curves by using sodium pyrophosphate. Phosphate (2  $\mu$ mol/L) is generated from 1  $\mu$ mol/L PPi and thus corresponds to 1  $\mu$ mol/L of generated UDP-GlcNAc. Data for patients and control subjects ( $n = 2$ ) were collected from 3 independent experiments. Error bars were used to indicate SDs. *P* values were calculated by using the Student *t* test.

## Flow cytometric analysis of GPI-anchored membrane proteins

For flow cytometric analysis of the expression of GPI-anchored membrane proteins, peripheral blood leukocytes were collected in Cyto-Chex-Blood Collection Tubes (Streck, Omaha, Neb) and stained with the following fluorochrome-labeled mouse anti-human mAbs (all from Beckman Coulter, Fullerton, Calif): CD59 (P282E), CD55 (JS11KSC2.3), CD24 (ALB9), CD14 (RMO52), and FLAER (Cedarlane, Burlington, Ontario, Canada) for expression level analysis and CD3 (UCHT1), CD4 (13B8.2 and SFCI12T4D11), CD16 (3G8), CD19 (J3.119), and CD45 (J.33) for gating. Cells were analyzed on a FACS Navios (Beckman Coulter) with Navios Software and FlowJo software (TreeStar, Ashland, Ore).

## Analysis of neutrophil chemotaxis

Polymorphonuclear lymphocyte migration was determined in a 2-chamber system with Fluoroblok inserts (3- $\mu$ m pore size; 24-well format; Falcon; Becton Dickinson, San Jose, Calif), as previously described.<sup>E12</sup> Cells were labeled with Calcein-AM and transferred to the upper chamber. The lower chamber contained chemoattractants (platelet-activating factor, IL-8, and C5a; 10 nmol/L each) or buffer alone. As a parameter of migrated polymorphonuclear lymphocytes, fluorescence increase in the lower compartment was measured every 2.5 minutes for a total of 45 minutes by using an EnVision reader (PerkinElmer, Hamburg, Germany). The maximal slope of migration was calculated over a 10-minute interval. Using this assay, we did not detect substantial differences in the maximal slope of migration between patients and control subjects.

## RESULTS

### Clinical assessments of the affected subjects

Family A (Fig 1, A) is a Tunisian family with 4 patients (A.V.12, A.V.13, A.V.14, and A.V.18). The first male patient, A.V.12, was born in 2000 to consanguineous parents. He presented at age 4 months with cutaneous suppurative lesions and recurrent pulmonary infections, including 3 episodes of pneumonia, as well as bronchiectasis. At age 6 years, he was still unable to walk and had otopyorrhea, pyodermititis of the scalp,

and several cutaneous abscesses. Developmental delay was observed but not formally tested. At the last follow-up at age 7 years, he had scoliosis (curvature 20°) and joint hyperextensibility, features consistent with HIES.<sup>E13</sup>

The second male patient, A.V.18, born to consanguineous parents in 2005, was first given a diagnosis at age 1 month with bronchitis and cutaneous erythematous lesions of the neck and back. At age 5 months, he presented with scalp pyodermititis, multiple cutaneous abscesses, and severe eczema. At age 1 year, he presented with multiple infected skin ulcers of the neck and trunk with isolation of *Staphylococcus aureus*, *Klebsiella pneumoniae*, *Enterococcus cloacae*, and *Streptococcus dysgalactiae equisimilis*. At age 2 years, he had mastoiditis and eczema on his face. At age 3 years, he was given a diagnosis of epilepsy, severe developmental delay, and generalized failure to thrive. He had hypotonia, being unable to sit through the last examination in 2011 at the age of 6 years and 2 months. He also had joint hyperextensibility.

His female first cousin (A.V.13) presented at age 7 months with generalized eczema. She was hospitalized at 10 months of age with impetigo and bronchitis. At 14 months of age, she died from septicemia associated with a severe bout of diarrhea.

Her twin sister, A.V.14, presented at 2 months with similar skin features, *S aureus* infection, and diffuse localization, including the trunk. At age 5 months, she had suppurative perichondritis of the right ear because of *Pseudomonas aeruginosa*, necessitating surgery. At age 9 months, she was hospitalized for *S aureus* septicemia secondary to infected skin lesions and persistent diarrhea. At the last follow-up at age 13 months, she continued to have recurrent bronchitis and oral candidiasis. Shortly after, she died at home, probably because of septicemia.

All patients of family A had height and weight below the third percentile at their last clinical examination. Additionally, 1 sibling in one of the branches of family A who died at the age of 2 and a half years was classified as having "Krabbe disease" (OMIM no. 245200), which is a fatal degenerative demyelization disorder.

A clinical description of family B was previously published as Buckley syndrome (ie, HIES).<sup>E14</sup> Affected subjects B.V.6 and B.V.7 were born in 1978 and 1980, respectively, to first-cousin Tunisian parents (Fig 1, B). Their older brother had subcutaneous abscesses and pyodermititis of the scalp and died at age 2 months after acute diarrhea. A sister, B.V.8, now 31 years old, is healthy and did not have any clinical features of HIES.

B.V.6 was 3 months old when presenting with weeping pyodermititis of the scalp. This was followed by eczema with cervicoaxillary and inguinal polyadenopathy and multiple subcutaneous abscesses. He presented at age 3 years with osteomyelitis of the shinbone, which was treated by means of immobilization, and a left-sided suppurative perinephritis requiring surgery. At age 5 years, he was hospitalized because of chronic rhinitis, bilateral otopyorrhea, and several episodes of chronic bronchitis. At age 6 years, a right-sided suppurative perinephritis again necessitated surgical intervention. He presented with weeping folliculitis on his scalp with impetiginization. Cultures from the scalp revealed *S aureus* and hemolytic *Streptococcus* group A. Eczema was present at the inguinal folds and intergluteal cleft. Variably sized nonsuppurative mastoidal, occipital, and axillary and jugular polyadenopathies were observed. He did not have hepatosplenomegaly or neurologic

disorders. B.V.6 is now 34 years old, with chronic obstructive pulmonary disease (emphysema) and bronchiectasis.

His brother, B.V.7, presented at age 4 months with milder clinical features. His disease started out with weeping dermatitis of the scalp, followed by cervical adenopathies and several episodes of bronchitis. Like his brother, he had pyodermititis of the scalp, infected eczema at inguinal folds, and inflamed polyadenopathies. *S aureus* was also isolated from the scalp. B.V.7 also had mild bronchiectasis. Both affected subjects had joint hyperextensibility. However, both had particularly characteristic faces, as has been described for AD-HIES with a typical facies, wide nostrils, and prominent lips.<sup>E14</sup> Both siblings had mild developmental delay, but this was not formally tested. Temporarily, both patients received IgG replacement therapy (intravenous immunoglobulin), although without improvement of their clinical condition.

The patient from Turkey (C.IV.7) was born to a family with several consanguineous marriages (Fig 1, C). At age 6.5 years, he was admitted to the hospital with complaints of fatigue, pallor, and darkening of urine. He had severe chicken pox and frequent pulmonary infections that required hospitalization 7 times. Initial physical examination showed tachycardia, jaundice, and generalized hypopigmented chicken pox scars. Additionally, thorax tomography revealed bronchiectasis. He successfully received intravenous immunoglobulin replacement to reduce the frequency of infections, although his IgG levels were normal. At the most recent clinical examination, he was 11.5 years old. He had generalized failure to thrive, with a weight of 20 kg (less than third percentile) and short stature of 112 cm (less than third percentile). He has mild developmental delay, as judged from psychometric tests. Epilepsy and focal neurologic deficit have not been observed. Results of magnetic resonance imaging was normal. Unlike some of the other patients, C.IV.7 walks normally and does not have scoliosis.

Family D originates from Morocco. Patients D.IV.2 and D.IV.5 were born in 1991 and 2001, respectively (Fig 1, D). D.IV.2 presented with eczema at 3 months of age that became generalized at 6 months of age. During the first year of life, D.IV.2 had otitis media, recurrent respiratory tract infections, and cold abscesses. He never had a fever during early childhood but produced purulent sputum since he was 10 years old. He is currently 21 years old, with severe growth retardation, mild mental retardation, and a characteristic dysmorphic facies. The patient presented with clubbing on the hands and feet and chest deformation, but he had no joint hyperextensibility or vertebral deformations. At his last chest computed tomographic scan, he had diffuse bronchial dilatation.

His brother, D.IV.5, presented with dermatitis at age 3 months and recurrent otitis since his first year of life. He had no cold abscesses, but at age 2 years, he presented with severe asthma. D.IV.5 is now 11 years old, and at his latest examination, he had erythematous-squamous lesions, temporoparietal alopecia plaques, asthma, and fever. His clinical symptoms are milder than those of his affected brother; he has no clubbing, no joint hyperextensibility, and no mental retardation. He had dysmorphic facies, although this was less evident than in his brother. The computed tomographic scan of his lungs showed bilateral bronchial dilatation.

## Analysis of T-cell subsets in patients with *PGM3* mutations

In patients with HIES, an imbalance of the  $T_{H1}/T_{H2}$  cytokine ratio has been proposed to account for recurrent infections. Therefore we analyzed the T-cell subsets in our *PGM3* cohort by using FACS measurements of cytokine responses after stimulation of purified PBMCs with PMA/ionomycin (Fig E1). Two patients were found to have increased proportions of  $T_{H2}$  cells (Table III). Because impaired  $T_{H17}$  cell function has been previously associated with HIES, we also asked whether the  $T_{H1}/T_{H17}$  ratio is impaired. Using IL-17/IFN- $\gamma$  staining, we found that the proportion of  $T_{H17}$  cells is comparable with control values. These results were confirmed in 2 patients from family A (p.Glu340del) who had normal IL-22 production (data not shown), indicating that no general  $T_{H17}$  defect is present. We finally observed a slightly diminished number of CD25<sup>high</sup>/forkhead box protein 3-positive regulatory T cells. T-cell subsets were also analyzed in close detail in the accompanying article by Zhang et al.<sup>E15</sup>

Using a carboxyfluorescein succinimidyl ester T-cell proliferation assay, we also determined the proportion of CD4<sup>+</sup> and CD8<sup>+</sup> cells in blood samples from the patient of family C. After stimulation with PHA, we found normal proliferation of CD4<sup>+</sup> but markedly reduced proliferation of CD8<sup>+</sup> T cells compared with those seen in a control subjects (Fig E2). After T-cell receptor-dependent stimulation, proliferation of both CD4<sup>+</sup> and CD8<sup>+</sup> T cells was almost absent.

In summary, our observations do not provide firm evidence that a  $T_{H17}$  defect is responsible for the HIES phenotype in our patients with *PGM3* mutations. However, the unusual expansion of the  $T_{H2}$  cell population and the pronounced reduction in T-cell proliferation require further detailed investigation.

## REFERENCES

- E1. Glocker E-O, Hennigs A, Nabavi M, Schäffer AA, Woellner C, Salzer U, et al. A homozygous *CARD9* mutation in a family with susceptibility to fungal infections. *N Engl J Med* 2009;361:1727-35.
- E2. Lathrop GM, Lalouel JM, Julier C, Ott J. Strategies for multilocus analysis in humans. *Proc Natl Acad Sci U S A* 1984;81:3443-6.
- E3. Cottingham RW Jr, Idury RM, Schäffer AA. Faster sequential genetic linkage computations. *Am J Hum Genet* 1993;53:252-63.
- E4. Schäffer AA, Gupta SK, Shriram K, Cottingham RW Jr. Avoiding recomputation in linkage analysis. *Hum Hered* 1994;44:225-37.
- E5. Stenberg J, Dahl F, Landegren U, Nilsson M. PieceMaker: selection of DNA fragments for selector-guided multiplex amplification. *Nucleic Acids Res* 2005;33:e72.
- E6. Stenberg J, Zhang M, Ji H. Disperse—a software system for design of selector probes for exon resequencing applications. *Bioinformatics* 2009;25:666-7.
- E7. Johansson H, Isaksson M, Falk-Sörqvist E, Roos F, Stenberg J, Sjöblom T, et al. Targeted resequencing of candidate genes using selector probes. *Nucleic Acids Res* 2011;39:e8.
- E8. Stenberg J, Nilsson M, Landegren U. ProbeMaker: an extensible framework for design of sets of oligonucleotide probes. *BMC Bioinformatics* 2005;6:229.
- E9. Ng PC, Henikoff S. Accounting for human polymorphisms predicted to affect protein function. *Genome Res* 2002;12:436-46.
- E10. Ceroni A, Maass K, Geyer H, Geyer R, Dell A, Haslam SM. GlycoWorkbench: a tool for the computer-assisted annotation of mass spectra of glycans. *J Proteome Res* 2008;7:1650-9.
- E11. Mio T, Yamada-Okabe T, Arisawa M, Yamada-Okabe H. Functional cloning and mutational analysis of the human cDNA for phosphoacetylglucosamine mutase: identification of the amino acid residues essential for the catalysis. *Biochim Biophys Acta* 2000;1492:369-76.

- E12. Kenzel S, Mergen M, von Süßkind-Schwendi J, Wennekamp J, Deshmukh SD, Haeffner M, et al. Insulin modulates the inflammatory granulocyte response to streptococci via phosphatidylinositol 3-kinase. *J Immunol* 2012; 189:4582-91.
- E13. Grimbacher B, Holland SM, Gallin JI, Greenberg F, Hill SC, Malech HL, et al. Hyper-IgE syndrome with recurrent infections—an autosomal dominant multisystem disorder. *N Engl J Med* 1999;340:692-702.
- E14. Ayed K, Ben Dridi MF, Gorgi Y, Bardi R, Hamzaoui K, Dali S. Forme familiale du syndrome de Buckley avec anomalies de l'immunité cellulaire [Familial form of the Buckley syndrome with anomalies of cellular immunity]. *Ann Pediatr* 1987;34:645-8.
- E15. Zhang Y, Yu X, Ichikawa M, Lyons JJ, Datta S, Lamborn IT, et al. Autosomal recessive phosphoglucomutase 3 (*PGM3*) mutations link glycosylation defects to atopy, immune deficiency, autoimmunity, and neurocognitive impairment. *J Allergy Clin Immunol* 2014 doi:10.1016/j.jaci.2014.02.013.
- E16. Babu P, North SJ, Jang-Lee J, Chalabi S, Mackerness K, Stowell SR, et al. Structural characterization of neutrophil glycans by ultra sensitive mass spectrometric glycomics methodology. *Glyconj J* 2009;26:975-86.

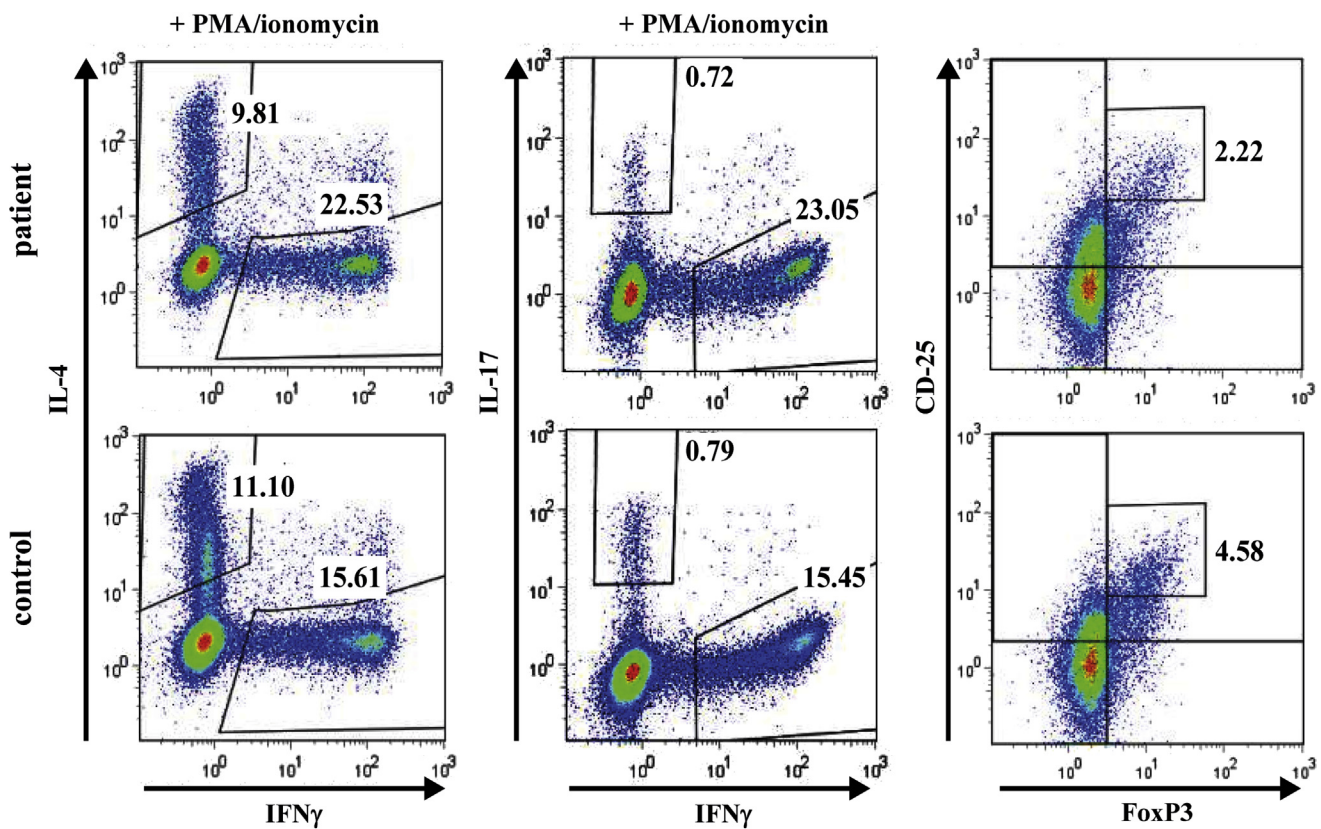


**FIG E1.** T<sub>H</sub>2 skewing but normal T<sub>H</sub>17 cell numbers in a patient with *PGM3* mutations. Freshly isolated PBMCs from patient B.V.6 were stimulated, and cytokine profiles were determined by using FACS analysis, as indicated. *Left panels:* upper left gate, IL-4-producing T<sub>H</sub>2 cells; lower right gate, IFN- $\gamma$ -producing T<sub>H</sub>1 cells. *Middle panels:* upper left gate, IL-17-producing T<sub>H</sub>17 cells; lower right gate, IFN- $\gamma$ -producing T<sub>H</sub>1 cells. *Right panels:* Gate shows the proportion of CD25<sup>high</sup>/forkhead box protein 3 (*FoxP3*)<sup>+</sup> regulatory T cells.

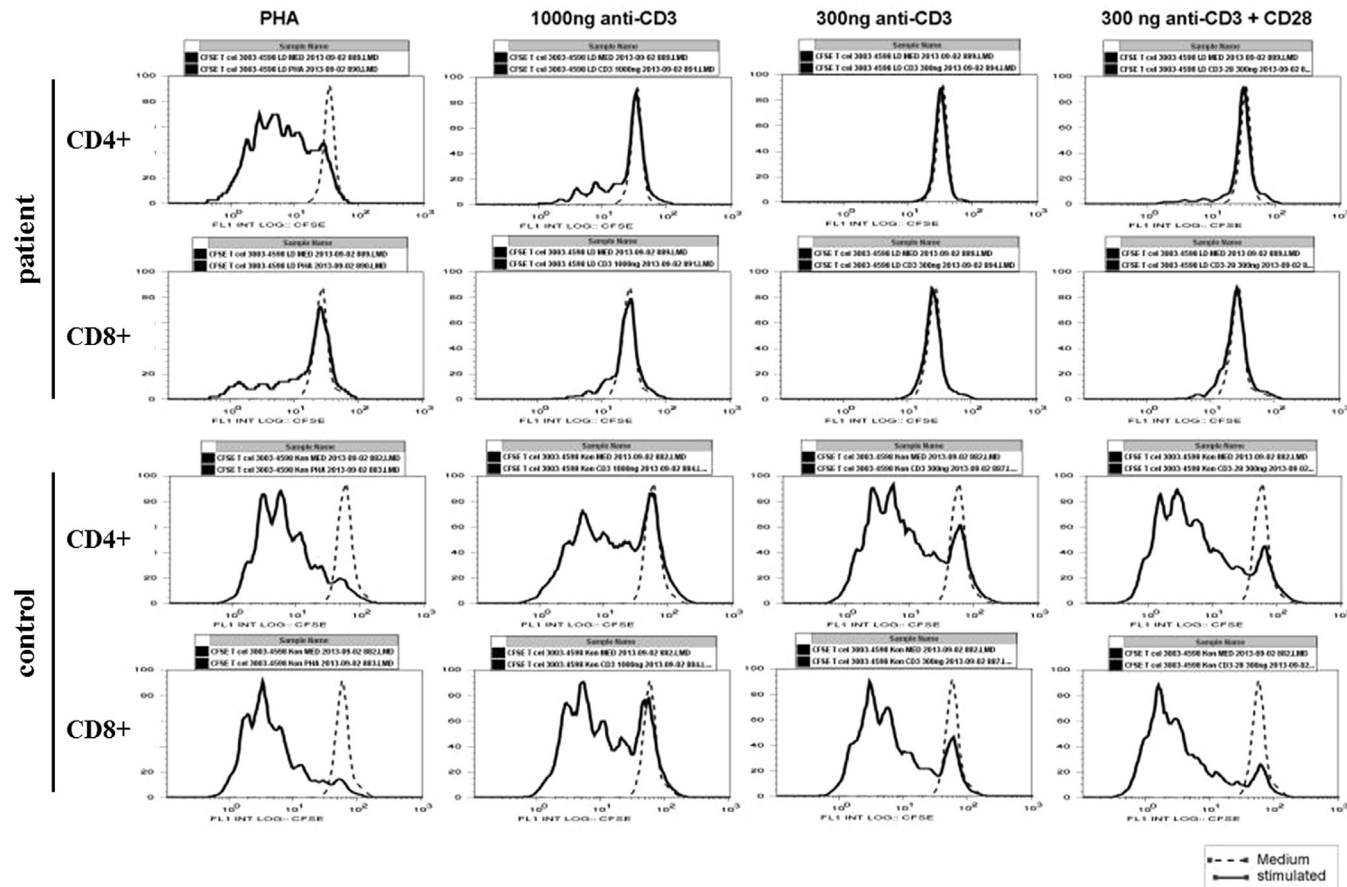


**FIG E2.** Impaired T-cell proliferation in a patient with *PGM3* mutations. Freshly isolated PBMCs from C.IV.7 were subjected to a carboxyfluorescein succinimidyl ester T-cell proliferation assay. *Left panels:* Normal proliferation of CD4<sup>+</sup> T cells but diminished proliferation of CD8<sup>+</sup> T cells after stimulation with PHA. *Right panels:* Almost absent proliferation of both CD4<sup>+</sup> and CD8<sup>+</sup> T cells on regulatory T cell-dependent stimulation with anti-CD3 and anti-CD28.

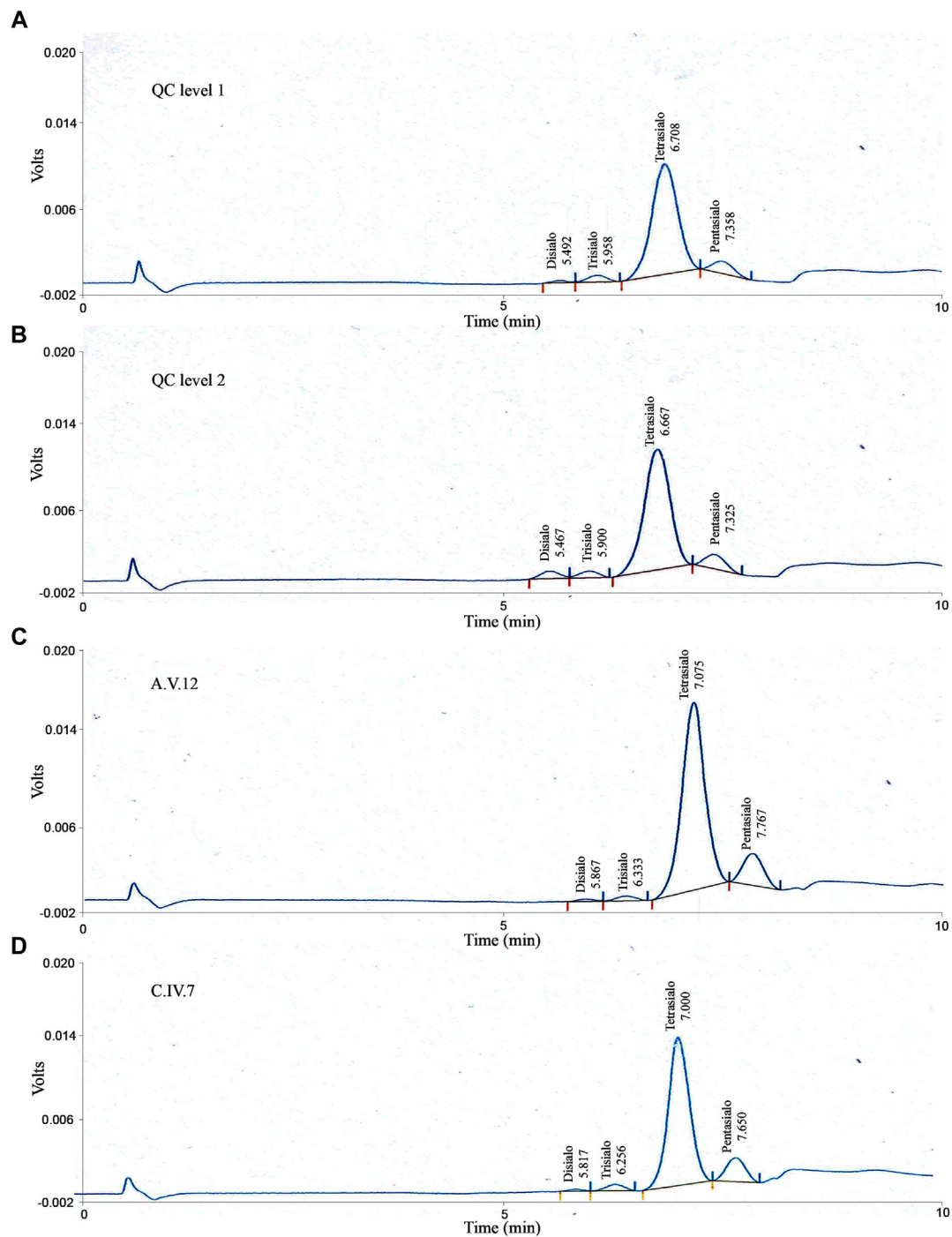


**FIG E3.** Normal transferrin glycoform patterns in sera from patients with *PGM3* mutations. **A** and **B**, Asialo-, mono-, di-, tri-, tetra-, and pentasialo-transferrin glycoform patterns in a control serum were analyzed by using HPLC (quality control [QC] level 1 and 2). **C** and **D**, Normal HPLC chromatograms demonstrate normal relative distribution of transferrin glycoforms in sera from patients carrying *PGM3* mutations: A.V.12 (p.Glu340Del) and C.IV.7 (p.Asp502Tyr). Transferrin carries 2 bi-antennary N-linked glycans with terminal sialic acid residues, which are used for diagnostic testing for CDGs. Defective transferrin glycosylation would be indicated by an increase of at least one of the asialotransferrin, mono-sialotransferrin, di-sialotransferrin, or tri-sialotransferrin glycoform levels and a decrease in tetra-sialotransferrin levels.

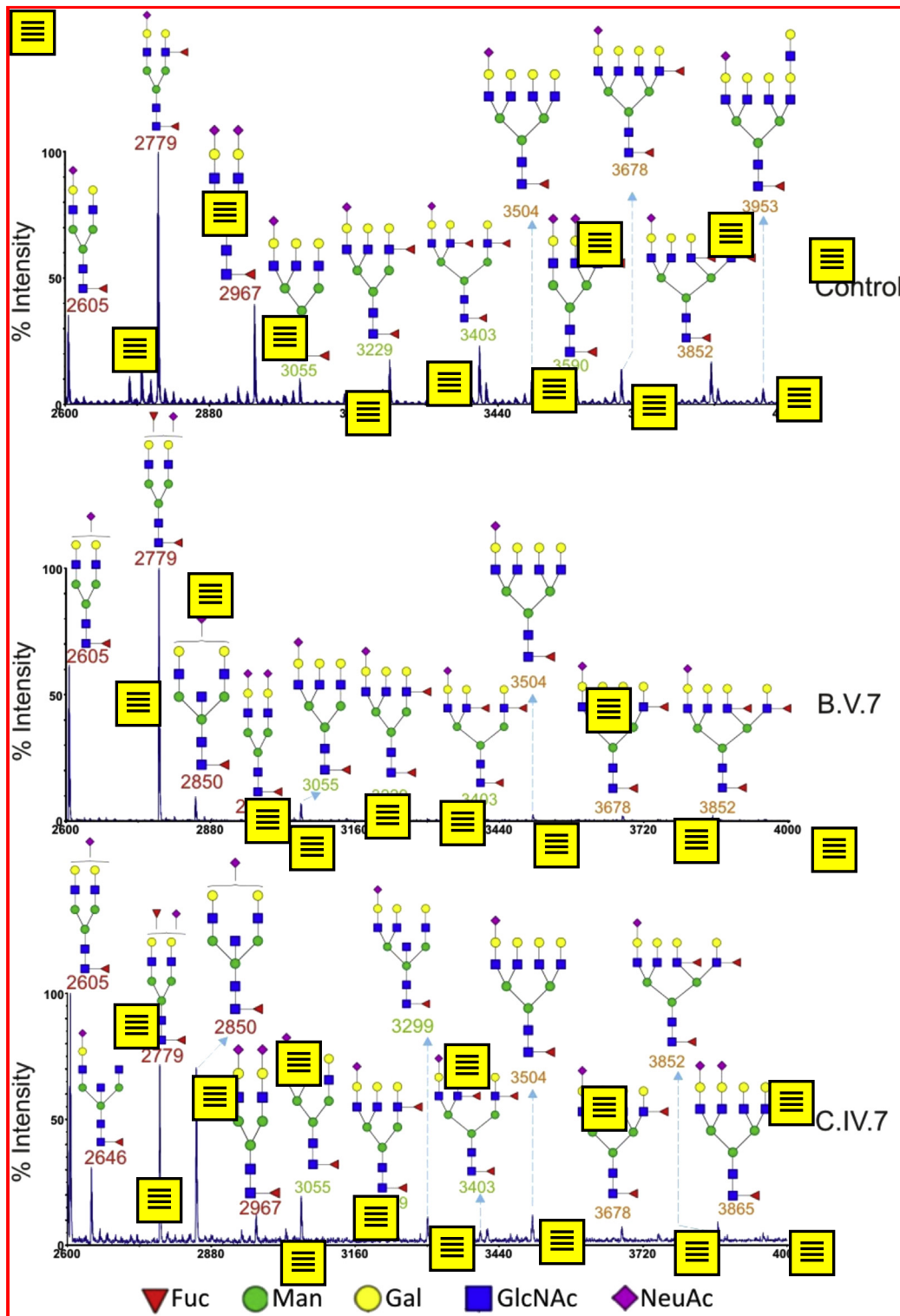


**FIG E4.** Accumulation of bi-antennary N-glycans in neutrophils from patients with *PGM3* mutations. Mass spectra of permethylated N-glycans of neutrophils from a healthy control subject and the affected subjects B.V.7 and C.IV.7. Results are summarized in Fig 4, B, with consistent color codes. Glycomic data of the control is from Babu et al.<sup>E16</sup>

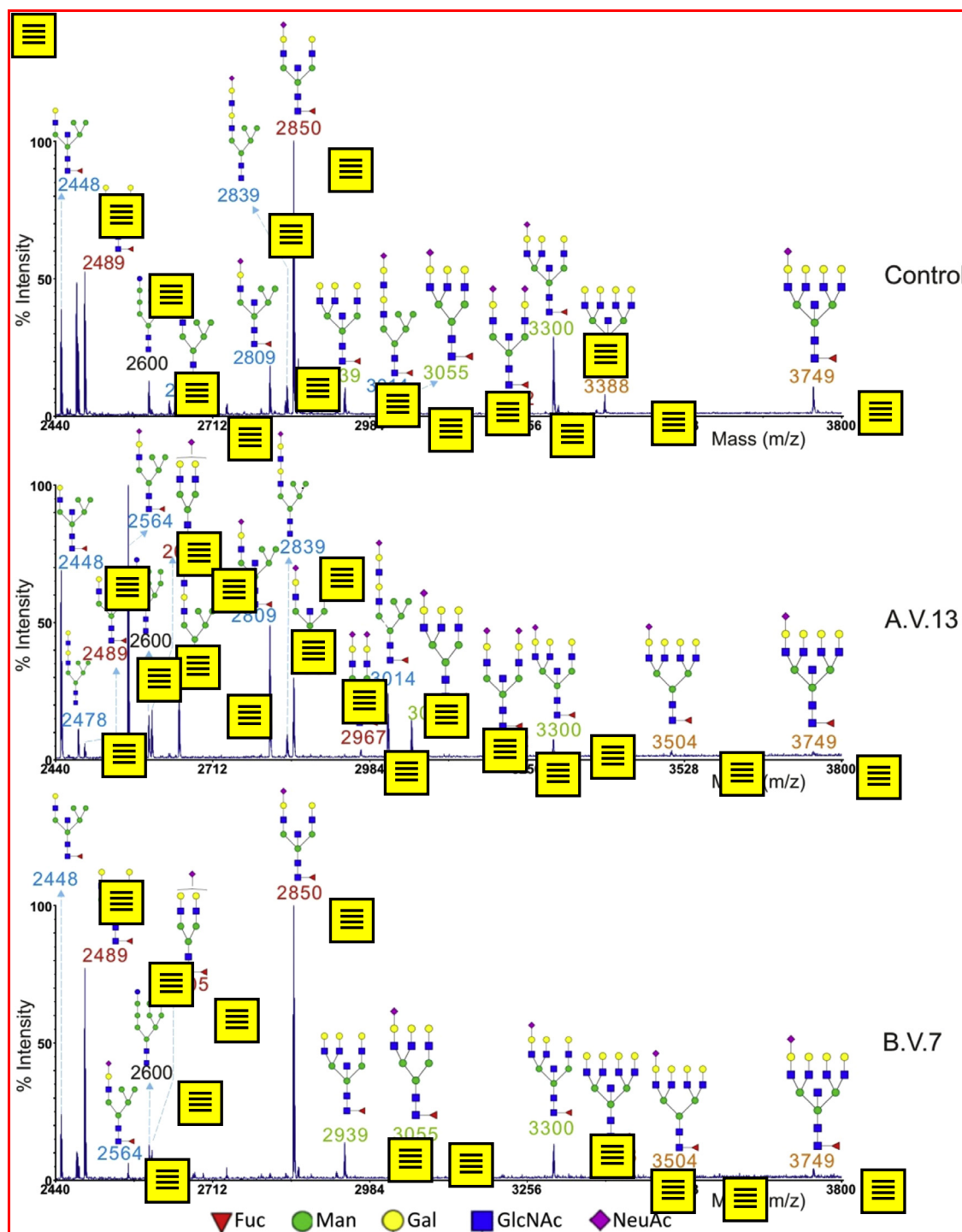


**FIG E5.** The p.Glu340del mutation causes accumulation of hybrid-type glycans. Mass spectra of permethylated N-glycans from EBV-transformed B cells from a healthy control subject and the affected subjects A.V.13 and B.V.7. Accumulation of hybrid glycans with a simultaneous decrease in tri-antennary and tetra-antennary glycan levels in B cells from affected subject A.V.13 (p.Glu340del mutation in the sugar-binding domain). Similarly, as observed in neutrophils, B cells from patient B.V.7 (p.Leu83Ser; catalytic domain) have decreased tri-antennary and tetra-antennary glycan levels, whereas bi-antennary N-glycan levels are increased. Results are summarized in Fig 4, C, with consistent color codes.

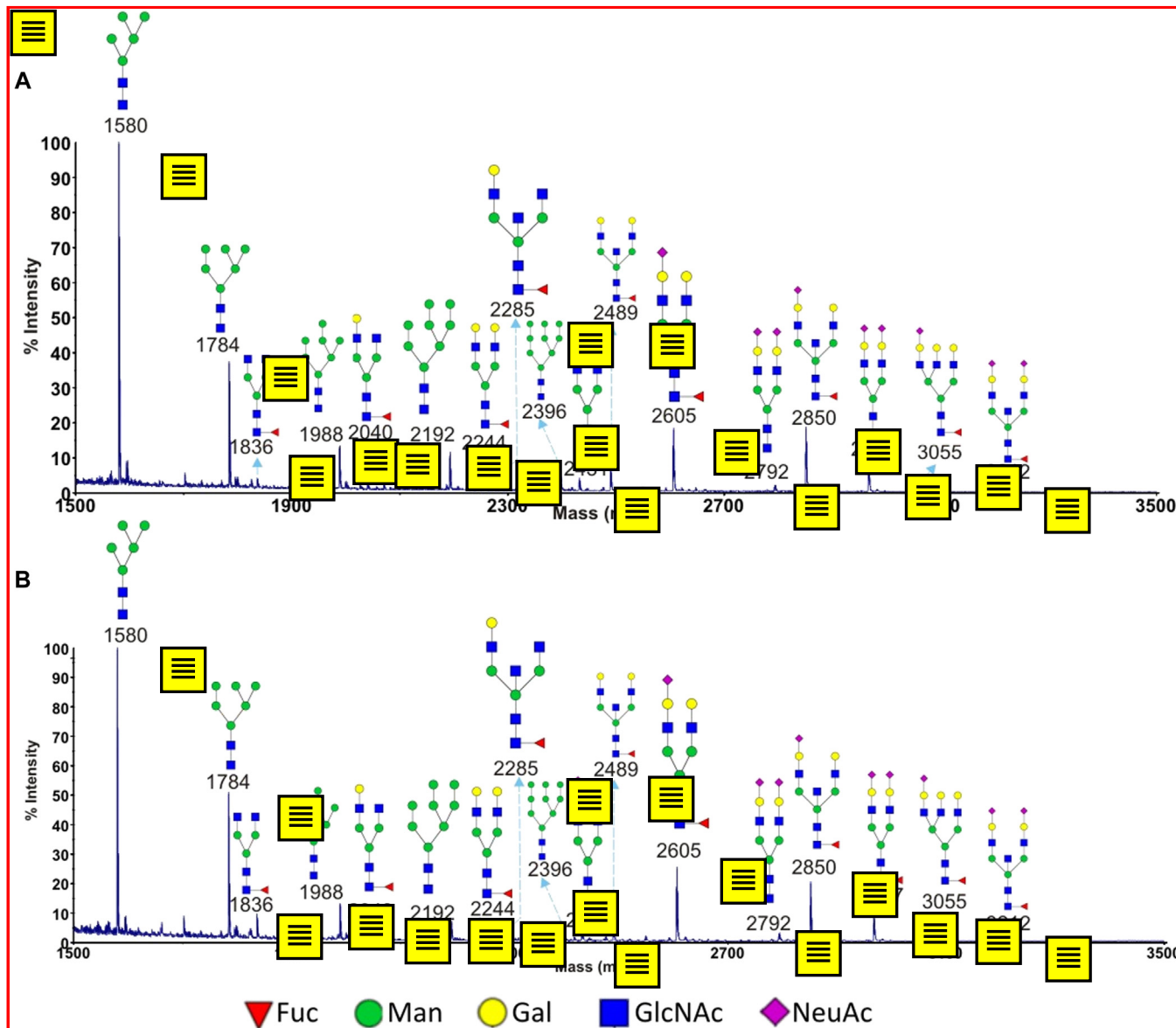


**FIG E6.** No significant alterations of the IgE N-glycan profile in a patient with *PGM3* mutations. **A**, Matrix-assisted laser desorption/ionization time-of-flight mass spectra of permethylated N-glycans from IgE from an affected subject from family A (p.Glu340del). **B**, Patient with atopic dermatitis as a control subject (serum IgE levels in healthy subjects is low). All molecular ions are  $[M^+Na]^+$ . Putative structures are based on composition, tandem mass spectrometry, and the biosynthetic pathway. Differences (fold intensities) were observed for glycans with the following masses—decreased in patient with *PGM3* mutation: 1784, 0.73 $\times$ ; 1836, 0.50 $\times$ ; 2040, 0.33 $\times$ ; 2244, 0.67 $\times$ ; 2605, 0.67 $\times$ ; 2792, 0.67 $\times$ ; increased in patient with *PGM3* mutation: 2192, 1.50 $\times$ ; 2285, 1.67 $\times$ ; 2396, 1.40 $\times$ ; 3212, 1.50 $\times$ . Decreases mainly affect complex-type glycans (bi-antennary), whereas increases affect high-mannose and hybrid-type glycans. Whether these subtle differences have functional consequences is currently not known. Exceptional peaks did not occur.

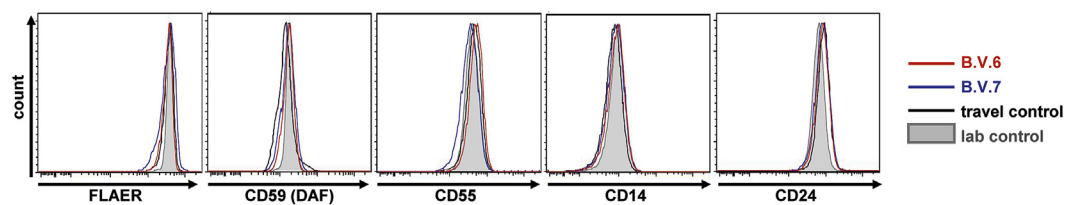


**FIG E7.** Normal expression of GPI-anchored membrane proteins on peripheral blood leukocytes from patients with *PGM3* mutations. Normal expression of CD59, CD55 (DAF), CD24, CD14, and FLAER on granulocytes of the patients of family B (red and blue) compared with a travel control (black) and a laboratory control (gray filled).

**TABLE E1.** Genes in the interval chr6:73.2-85.1Mb (build 36/hg18 coordinates) analyzed by using Sanger sequencing (indicated by asterisks) or high-throughput sequencing (all)

Gene symbol	Full gene name
<i>BCKDHB</i>	Branched chain keto acid dehydrogenase E1, beta polypeptide
<i>C6orf150</i>	Chromosome 6 open reading frame 150
<i>C6orf221</i>	Chromosome 6 open reading frame 221
<i>CD109*</i>	CD109 molecule
<i>COL12A1</i>	Collagen, type XII, alpha 1
<i>COX7A2</i>	Cytochrome c oxidase subunit VIIa polypeptide 2 (liver)
<i>CYB5R4</i>	Cytochrome b5 reductase 4
<i>DDX43</i>	DEAD (Asp-Glu-Ala-Asp) box polypeptide 43
<i>DOPEY1*</i>	Dopey family member 1
<i>DPPA5</i>	Developmental pluripotency associated 5
<i>EEF1A1</i>	Eukaryotic translation elongation factor 1 alpha 1
<i>ELOVL4</i>	Elongation of very long chain fatty acids (FEN1/Elo2, SUR4/Elo3, yeast)-like 4
<i>FAM46A</i>	Family with sequence similarity 46, member A
<i>FILIP1</i>	Filamin A interacting protein 1
<i>HMGN3</i>	High mobility group nucleosomal binding domain 3
<i>HTR1B</i>	5-Hydroxytryptamine (serotonin) receptor 1B
<i>IBTK*</i>	Inhibitor of Bruton agammaglobulinemia tyrosine kinase
<i>IMPG1</i>	Interphotoreceptor matrix proteoglycan 1
<i>IRAK1BP1*</i>	IL-1 receptor-associated kinase 1 binding protein 1
<i>KCNQ5</i>	Potassium voltage-gated channel, KQT-like subfamily, member 5
<i>KHDC1</i>	KH homology domain containing 1
<i>KHDC1L</i>	KH homology domain containing 1-like
<i>KIAA1009</i>	KIAA1009
<i>LCA5</i>	Leber congenital amaurosis 5
<i>LOC100128859</i>	—
<i>LOC100129436</i>	—
<i>LOC100131508</i>	—
<i>ME1</i>	Malic enzyme 1, NADP(+) -dependent, cytosolic
<i>MRAP2</i>	Melanocortin 2 receptor accessory protein 2
<i>MTO1</i>	Mitochondrial translation optimization 1 homolog
<i>MYO6</i>	Myosin VI
<i>OOEP</i>	Oocyte expressed protein homolog
<i>PGM3</i>	Phosphoglucomutase 3
<i>PHIP</i>	Pleckstrin homology domain interacting protein
<i>PRSS35</i>	Protease, serine, 35
<i>RIPPLY2</i>	Ripply2 homolog
<i>RWDD2A</i>	RWD domain containing 2A
<i>SENPG*</i>	SUMO1/sentrin specific peptidase 6
<i>SH3BGRL2*</i>	SH3 domain binding glutamic acid-rich protein like 2
<i>SLC17A5</i>	Solute carrier family 17 (anion/sugar transporter), member 5
<i>SNAP91</i>	Synaptosomal-associated protein, 91kDa homolog
<i>TMEM30A</i>	Transmembrane protein 30A
<i>TPBG</i>	Trophoblast glycoprotein
<i>TTK</i>	TTK protein kinase
<i>UBE2CBP</i>	Ubiquitin-conjugating enzyme E2C binding protein

The pseudogene *GAPDHL8* was not sequenced.

\*Genes analyzed by Sanger sequencing.

**TABLE E2.** Mutations observed in *PGM3*, their effects on the different protein isoforms, transcript variants, and the corresponding dbSNP identifiers

Origin	Family A: Tunisia	Family B: Tunisia	Family C: Turkey	Family D: Morocco
Effect on PGM variants 001 and 004	p.Glu340del c.1018_1020del	p.Leu83Ser c.248T>C	p.Asp502Tyr c.1504G>T	p.Leu83Ser c.248T>C
Effect on PGM variant 002	p.Glu368del c.1102_1104del	p.Leu111Ser c.332T>C	p.Asp530Tyr c.1588G>T	p.Leu111Ser c.332T>C
dbSNP id	rs267608259 exon 9	rs267608260 exon 4	rs267608261 exon 13	rs267608260 exon 4

All 3 mutated positions also occur in the shorter isoform PGM-003, which is not shown because of inconsistent entries in Ensembl and Entrez.